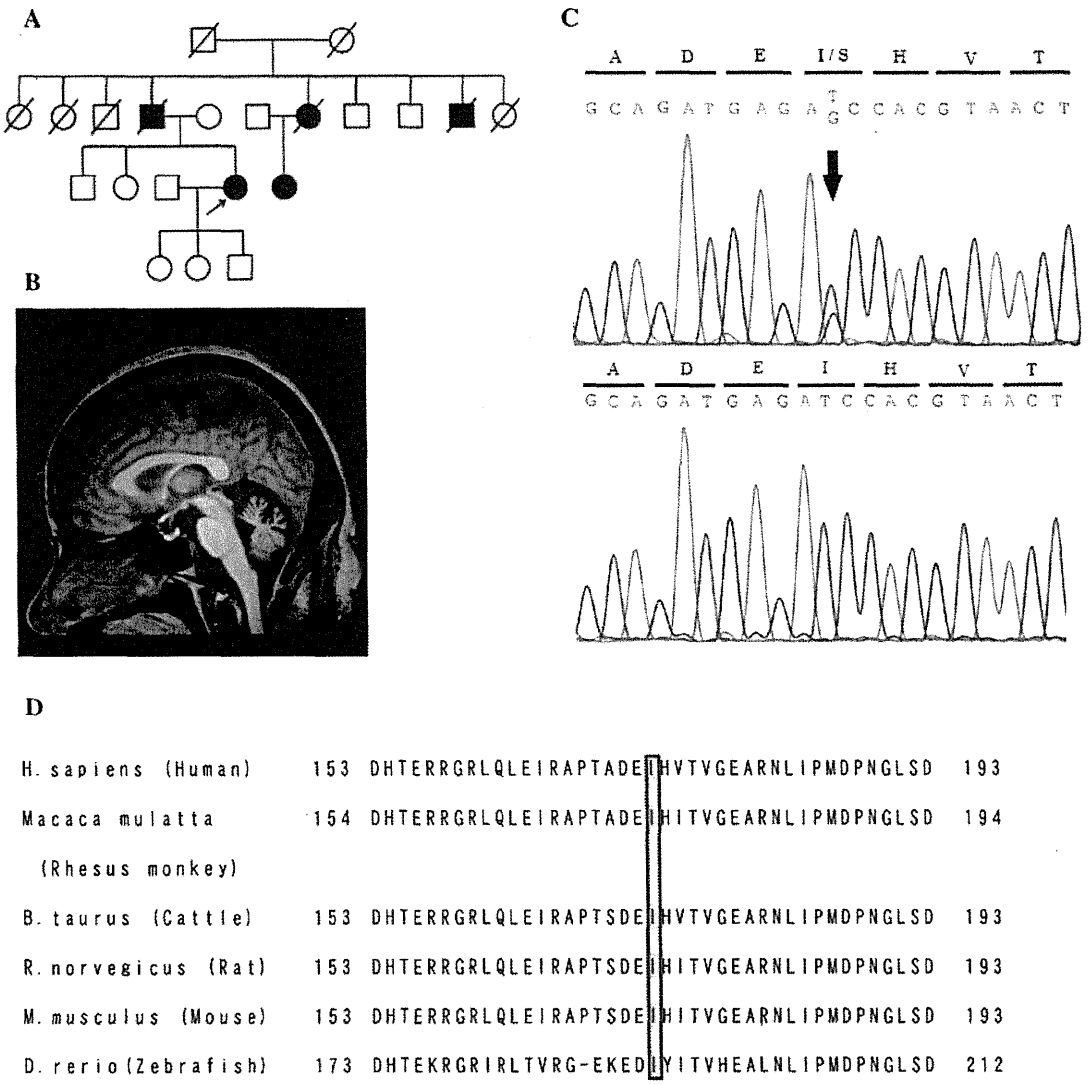

Fig. 1 **a** Family tree of the presented case. Autosomal dominant inheritance is indicated. **b** Sagittal view of T1 weighted magnetic resonance imaging in this patient shows marked atrophy in the upper cerebellum. **c** Sequencing analysis of exon five in PRKCG. The patient (*upper column*) has heterozygous c.518T>G substitution (p.Ile173Ser) whereas normal control (*lower column*) has no mutation. **d** The amino acid p.Ile173 residue is conserved among PRKCG proteins from mammals and zebrafish

(PolyPhen-2, http://genetics.bwh.harvard.edu/pph2/) and MutationTaster (http://www.mutationtaster.org). These programs predicted p.Ile173Ser to be 'damaging', 'possibly damaging' and 'disease causing', respectively. This novel mutation was located in the C2 domain of the PKCγ protein, which comprises amino acids 172–275 [5].

Since the first description of SCA14-causative mutations in *PRKCG* in 2003 [5], over 20 mutations have been reported. As mentioned above, most mutations lie in the C1 domain, which contributes to the localization of the protein. In contrast, no mutations had been found in the C2 domain, which functions as a Ca^{2+} sensor. Both these domains play an important role in the maintenance of Ca^{2+} homeostasis [6]. This novel mutation (p.Ile173Ser) may change protein function by altering its chemical properties from hydrophobic to hydrophilic. It is expected that this novel mutation will facilitate our understanding of PKCγ function and SCA14 pathogenesis.

Acknowledgments We thank the members of our laboratory, especially Ms. Ando Y., for genetic testing.

Conflicts of interest All authors report no conflicts of interest.

Ethical standard This study has been approved by the appropriate ethics committee and has, therefore, been performed in accordance with the ethical standards laid down in the 1964 Declaration of Helsinki.

References

1. Durr A (2010) Autosomal dominant cerebellar ataxias: polyglutamine expansions and beyond. Lancet Neurol 9:885–894
2. Klebe S, Durr A, Rentschler A, Hahn-Barma V, Abele M, Bouslam N, Schöls L, Jedynak P, Forlani S, Denis E, Dussert C, Agid Y, Bauer P, Globas C, Wüllner U, Brice A, Riess O, Stevanin G (2005) New mutations in protein kinase C gamma associated with spinocerebellar ataxia type 14. Ann Neurol 58:720–729
3. Dalski A, Mitulla B, Bürk K, Schattenfroh C, Schwinger E, Zühlke C (2006) Mutation of the highly conserved cysteine residue 131 of the SCA14 associated PRKCG gene in a family with slow progressive cerebellar ataxia. J Neurol 253:1111–1112
4. Koht J, Stevanin G, Durr A, Mundwiller E, Brice A, Tallaksen CM (2012) SCA14 in Norway, two families with autosomal dominant cerebellar ataxia and a novel mutation in the PRKCG gene. Acta Neurol Scand 125:116–122
5. Chen DH, Brkanac Z, Verlinde CL, Tan XJ, Bylenok L, Nochlin D, Matsushita M, Lipe H, Wolff J, Fernandez M, Cimino PJ, Bird TD, Raskind WH (2003) Missense mutations in the regulatory domain of PKC gamma: a new mechanism for dominant nonepisodic cerebellar ataxia. Am J Hum Genet 72:839–849
6. Adachi N, Kobayashi T, Takahashi H, Kawasaki T, Shirai Y, Ueyama T, Matsuda T, Seki T, Sakai N, Saito N (2008) Enzymological analysis of mutant protein kinase Cgamma causing spinocerebellar ataxia type 14 and dysfunction in Ca^{2+} homeostasis. J Biol Chem 283:19854–19863

Human Molecular Genetics, 2013, Vol. 22, No. 15 **3003–3015**
doi:10.1093/hmg/ddt157
Advance Access published on April 4, 2013

Impaired viability of muscle precursor cells in muscular dystrophy with glycosylation defects and amelioration of its severe phenotype by limited gene expression

Motoi Kanagawa[1], Chih-Chieh Yu[1,†], Chiyomi Ito[1,†], So-ichiro Fukada[2], Masako Hozoji-Inada[1], Tomoko Chiyo[3], Atsushi Kuga[1], Megumi Matsuo[1], Kanoko Sato[1], Masahiko Yamaguchi[2], Takahito Ito[2], Yoshihisa Ohtsuka[1], Yuki Katanosaka[4], Yuko Miyagoe-Suzuki[3], Keiji Naruse[4], Kazuhiro Kobayashi[1], Takashi Okada[3], Shin'ichi Takeda[3] and Tatsushi Toda[1,*]

[1]Division of Neurology/Molecular Brain Science, Kobe University Graduate School of Medicine, Kobe 650-0017, Japan, [2]Laboratory of Molecular and Cellular Physiology, Graduate School of Pharmaceutical Sciences, Osaka University, Suita 565-0871, Japan, [3]Department of Molecular Therapy, National Institute of Neuroscience, National Center of Neurology and Psychiatry, Kodaira 187-8502, Japan and [4]Department of Cardiovascular Physiology, Graduate School of Medicine, Dentistry and Pharmaceutical Sciences, Okayama University, Okayama 700-8558, Japan

Received January 7, 2013; Revised March 3, 2013; Accepted April 2, 2013

A group of muscular dystrophies, dystroglycanopathy is caused by abnormalities in post-translational modifications of dystroglycan (DG). To understand better the pathophysiological roles of DG modification and to establish effective clinical treatment for dystroglycanopathy, we here generated two distinct conditional knock-out (cKO) mice for *fukutin*, the first dystroglycanopathy gene identified for Fukuyama congenital muscular dystrophy. The first dystroglycanopathy model—myofiber-selective fukutin-cKO [muscle creatine kinase (MCK)-fukutin-cKO] mice—showed mild muscular dystrophy. Forced exercise experiments in presymptomatic MCK-fukutin-cKO mice revealed that myofiber membrane fragility triggered disease manifestation. The second dystroglycanopathy model—muscle precursor cell (MPC)-selective cKO (Myf5-fukutin-cKO) mice—exhibited more severe phenotypes of muscular dystrophy. Using an isolated MPC culture system, we demonstrated, for the first time, that defects in the fukutin-dependent modification of DG lead to impairment of MPC proliferation, differentiation and muscle regeneration. These results suggest that impaired MPC viability contributes to the pathology of dystroglycanopathy. Since our data suggested that frequent cycles of myofiber degeneration/regeneration accelerate substantial and/or functional loss of MPC, we expected that protection from disease-triggering myofiber degeneration provides therapeutic effects even in mouse models with MPC defects; therefore, we restored fukutin expression in myofibers. Adeno-associated virus (AAV)-mediated rescue of fukutin expression that was limited in myofibers successfully ameliorated the severe pathology even after disease progression. In addition, compared with other gene therapy studies, considerably low AAV titers were associated with therapeutic effects. Together, our findings indicated that fukutin-deficient dystroglycanopathy is a regeneration-defective disorder, and gene therapy is a feasible treatment for the wide range of dystroglycanopathy even after disease progression.

*To whom correspondence should be addressed at: 7-5-1 Kusunoki-chou Chuo-ku, Kobe 650-0017, Japan. Tel: +81 783826287; Fax: +81 783826288; Email: toda@med.kobe-u.ac.jp
†These authors contributed equally to this work.

INTRODUCTION

Dystroglycanopathy includes Walker–Warburg syndrome, muscle–eye–brain disease, Fukuyama congenital muscular dystrophy (FCMD) and several forms of congenital and limb–girdle muscular dystrophies (1). Dystroglycanopathy is indicated by a wide variety of clinical symptoms; the most severe end of the clinical spectrum is characterized by congenital muscular dystrophy with severe structural brain and eye abnormalities, whereas the mildest end presents in adult life with limb–girdle muscular dystrophy without brain or eye involvement (1). FCMD is the first dystroglycanopathy to be reported (2,3), and it is the second most common childhood muscular dystrophy in Japan. The founder mutation, a SINE-VNTR-*Alu* retrotransposon insertion in the 3′ noncoding region of *fukutin*, causes abnormal splicing that leads to the production of non-functional proteins in FCMD (4,5). FCMD is characterized by severe congenital muscular dystrophy, abnormal neuronal migration associated with mental retardation and epilepsy and, frequently, eye abnormalities. It often results in early death before the age of 20 (6). Several point mutations in *fukutin* have also been reported to be associated with dystroglycanopathy in Japan and other countries (7,8).

More than 10 genes [protein *O*-mannosyltransferase 1 (*POMT1*), protein *O*-mannosyltransferase 2 (*POMT2*), protein *O*-linked mannose β-1,2-*N*-acetylglucosaminyltransferase 1 (*POMGNT1*), *fukutin*, fukutin-related protein (*FKRP*), *LARGE*, dolichol-phosphate-mannose synthase (*DPM2* and *DPM3*), isoprenoid synthase domain containing (*ISPD*) gene, glycosyltransferase-like domain containing 2 (*GTDC2*) gene and β-1,3-*N*-acetylglucosaminyltransferase 1 (*B3GNT1*)], implicated in dystroglycanopathies, have been shown or expected to be involved in the glycosylation pathway of α-dystroglycan (α-DG) (1,9,10). POMGnT1 and the POMT1/2 complex possess glycosyltransferase activities and can directly synthesize *O*-mannosyl sugar chains on α-DG (11,12). Fukutin, FKRP and LARGE are involved in a novel phosphodiester-linked modification, namely, a post-phosphoryl modification, of *O*-mannose on α-DG (13,14). Recently, it has been shown that LARGE can act as a bifunctional glycosyltransferase with both xylosyltransferase and glucuronyltransferase activities (15). The DG gene *DAG1* encodes both α- and β-DG, which is post-translationally cleaved into the two subunits (16). α-DG is a highly glycosylated protein and serves as the receptor subunit for extracellular proteins such as laminins, perlecan, agrin, neurexin and pikachurin (9,17). *O*-mannosyl glycosylation and the post-phosphoryl modification are required for the ligand-binding activities of α-DG (3,13). Hypoglycosylation and reduced ligand-binding activity of α-DG are common characteristics of dystroglycanopathy. α-DG is anchored to the plasma membrane through non-covalent interactions with the transmembrane subunit β-DG. β-DG intracellularly interacts with dystrophin, whose mutations lead to Duchenne/Becker muscular dystrophy, and dystrophin, in turn, binds to actin filaments. This molecular linkage, created by laminin-DG-dystrophin-actin filaments, is thought to provide mechanical stability to the plasma membrane of the muscle fiber; thus, disruption of this linkage is considered a key pathological event in several forms of muscular dystrophy. In FCMD skeletal muscles, in addition to dystrophic muscular changes, there are certain characteristics such as intensive connective tissue infiltration and the presence of predominant small-sized fibers from the early infantile stage (6). Furthermore, aberrant neuromuscular junctions and delayed muscle fiber maturation have been implicated in the pathology of FCMD (18). FCMD also shows central nervous system involvement. Together, these data suggest that more complex and unknown physiological roles of α-DG modification underlie the skeletal muscle pathology of dystroglycanopathy.

Recent studies have identified new genes associated with dystroglycanopathy (19–21), and an increasing number of patients are being diagnosed with dystroglycanopathy worldwide. However, the pathogenesis of this condition is not fully understood, and no effective clinical treatment has been established. To understand the pathogenesis and establish a therapeutic strategy for dystroglycanopathy, we developed two distinct *fukutin* conditional knock-out (cKO) mice as models for dystroglycanopathy. In our study, investigation of presymptomatic fukutin-deficient mice provided direct evidence that fragility of the myofiber membrane triggers the pathogenesis of dystroglycanopathy. We also used an isolated muscle precursor cell (MPC) culture system to demonstrate, for the first time, that defects in the fukutin-dependent modification of DG lead to impairment of MPC proliferation, differentiation and muscle regeneration. We predicted that protection from disease-triggering myofiber degeneration would prevent substantial and/or functional loss of MPC, thereby providing therapeutic effects. Indeed, we demonstrate that restoration of fukutin expression in myofibers successfully ameliorates the severe pathology even after disease progression. These results indicate that gene therapy is a feasible treatment for dystroglycanopathy.

RESULTS

Generation and characterization of myofiber-selective fukutin cKO mice

To generate *fukutin*-cKO mice, flox fukutin mice (*fukutin*$^{lox/lox}$) were crossed with muscle creatine kinase (MCK)-Cre mice (22) or Myf5-Cre mice (23), which express the *Cre* gene with the help of the MCK promoter or Myf5 promoter, respectively (Supplementary Material, Fig. S1). The MCK promoter is active in differentiating and differentiated muscle cells (24), and MCK expression reaches maximum levels at post-natal day 10 and remains constantly high throughout life (25). First, we analyzed the MCK-fukutin-cKO mice at different time points. In the skeletal muscles of these mice, we confirmed dramatic reduction in the fukutin protein after the age of 4 weeks (Fig. 1A). Abnormal modification of α-DG is indicated by decreased molecular weight, loss of immunoreactivity against the monoclonal IIH6 antibody, which recognizes properly glycosylated α-DG (3), and decreased laminin-binding activity. Abnormally modified α-DG was predominant in MCK-fukutin-cKO mice aged >8 weeks (Fig. 1A). Loss of the post-phosphoryl modification was further confirmed by subjecting the protein to treatment with cold aqueous hydrofluoric (HF) acid, which cleaves phosphoester linkages, and to inorganic metal-affinity chromatography (IMAC), which captures monoester-linked phosphorylated compounds

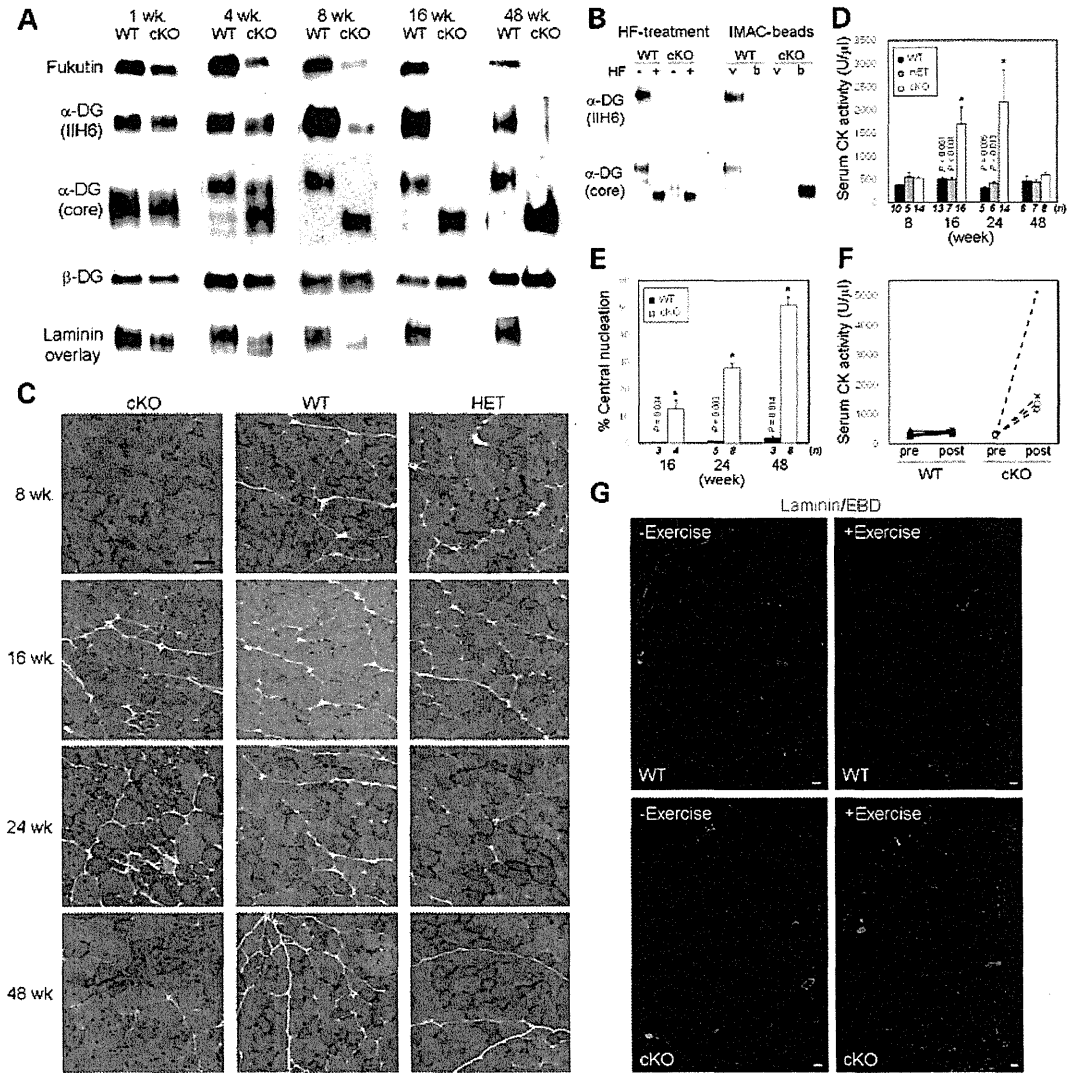

Figure 1. Pathological characterization of MCK-fukutin-cKO mice. **(A)** Western blot analysis of fukutin protein expression and α-DG modification in MCK-fukutin-cKO (cKO) and litter control WT skeletal muscles at different ages (1, 4, 8, 16 and 48 weeks). β-DG was used as a loading control. Laminin-binding activity of α-DG was examined by the laminin overlay assay. **(B)** Post-phosphoryl modification of α-DG from MCK-fukutin-cKO and control WT skeletal muscles. The absence of the post-phosphoryl modification was confirmed by HF treatment and IMAC-bead-binding assay. The void (v) and bound (b) fractions of the IMAC beads were analyzed by western blotting. **(C)** H&E staining of tibialis anterior muscles. Bar □50 μm. **(D)** Serum CK activity and **(E)** proportion of myofibers with centrally located nuclei. Data shown are mean ± SEM for each group (n is indicated in the graph). $^*P \leq 0.05$ for both cKO versus WT and cKO versus HET (D) and cKO versus WT (E) (Mann–Whitney U test; P-values are indicated in the graph). **(F)** Serum CK activity before and after forced exercise. Serum CK levels of individual mice (n □4 in each genotype) were measured before (pre) and after (post) exercise. **(G)** Uptake of Evans blue dye into myofibers after forced exercise. MCK-fukutin-cKO and control WT mice were subjected to forced exercise (+Exercise); subsequently, the muscle sections were stained with laminin (green) for individual fibers and merged with Evans blue dye (red). Mice not subjected to exercise were used as controls (−Exercise). Bar □200 μm.

(13,14). The molecular weight of α-DG in the skeletal muscles of control (WT) mice was dramatically reduced after HF treatment, and α-DG did not bind to IMAC beads because the phosphodiester-linked modification was intact; in contrast, α-DG in the skeletal muscles of MCK-fukutin-cKO mice showed little sensitivity to HF and bound to IMAC beads (Fig. 1B), indicating incomplete post-phosphoryl modification. Immunofluorescence staining with an antibody against an α-DG core protein showed that α-DG localized to the sarcolemma of MCK-fukutin-cKO mice as seen in normal controls (Supplementary Material, Fig. S2A), which suggests that cellular trafficking of α-DG is little affected by fukutin deficiency. These results confirmed abnormal modification of α-DG in the skeletal muscles of MCK-fukutin-cKO mice.

Hematoxylin and eosin (H&E) staining revealed that 16-week-old MCK-fukutin-cKO mice showed signs of muscular dystrophy, such as myonecrosis and central nucleation (Fig. 1C). Serum creatine kinase (CK) activity in

16-week-old MCK-fukutin-cKO mice was significantly higher than that in controls (Fig. 1D). These pathological features were not observed in 8-week-old mice (Fig. 1C and D); a possible reason may be the presence of residual α-DG with proper glycosylation (Supplementary Material, Fig. S2B). The population of myofibers with centrally located nuclei, an indication of repeated cycles of myofiber degeneration/regeneration, increased with age (Fig. 1E); however, more advanced pathology, such as infiltration of fat and connective tissues, was rarely observed even in 48-week-old MCK-fukutin-cKO mice (Fig. 1C).

It has been widely believed that functional and/or substantial loss of DG-containing protein complexes (i.e. the dystrophin–glycoprotein complex) leads to disease-causing membrane fragility. This concept is based on results of forced exercise experiments in animals with muscular dystrophy, which led to increases in the serum CK levels and uptake of membrane-impermeable Evans blue dye by myofibers (26,27). However, these experiments were conducted in diseased animals; therefore, it remains unclear whether membrane fragility triggers disease-causing phenotype. Therefore, we subjected 10-week-old MCK-fukutin-cKO mice, which showed abnormal α-DG modification but no pathology (Supplementary Material, Fig. S2C), to forced exercise. After forced exercise, serum CK levels were dramatically increased in the MCK-fukutin-cKO mice but not in the control mice (Fig. 1F). Myofibers with membrane-impermeable Evans blue dye uptake were also observed only in the exercise-administered MCK-fukutin-cKO mice (Fig. 1G). These data indicate that the plasma membrane of the muscle cells becomes weak before disease onset, providing proof-of-principle that membrane fragility triggers disease manifestation.

Characterization of MPC-selective fukutin cKO mice

Loss of fukutin in differentiated myofibers results in only mild and slow-progressing disease-causing phenotypes. We hypothesized that fukutin-dependent modification also plays a role in MPCs that are not targeted by MCK-Cre-mediated recombination. Therefore, we generated cKO mice lacking fukutin in MPCs by crossing flox fukutin mice with Myf5-Cre knock-in mice (23) expressing Cre recombinase under the control of the endogenous Myf5 promoter (Myf5-fukutin-cKO mice; Supplementary Material, Fig. S1). It has been reported that the Myf5-Cre allele recapitulates the expression pattern of the endogenous Myf5 gene and is uniformly expressed in all proliferating myoblasts (23). The Myf5-fukutin-cKO mice grossly show little difference compared with the litter controls until ~2 weeks of age; thereafter, increase in body weight was significantly retarded (Fig. 2A). Most Myf5-fukutin-cKO mice died by 6 months (Fig. 2B). Reduction in fukutin protein expression and abnormal modification were confirmed by immunofluorescence, western blotting, HF treatment and IMAC-bead assay (Fig. 2C and D). As is the case of MCK-fukutin-cKO, α-DG in Myf5-fukutin-cKO localizes to the sarcolemma (Supplementary Material, Fig. S2D). H&E staining revealed progressive pathological changes in Myf5-fukutin-cKO skeletal muscles (Fig. 2E). At 2 weeks, myonecrotic fibers were sparse (Supplementary Material, Fig. S2E), and at 4 weeks, in addition to myonecrotic fibers, myofibers with centrally located nuclei were observed (Fig. 2E). Serum CK levels and the proportion of the myofibers with centrally located nuclei were significantly higher in Myf5-fukutin-cKO mice than in the controls at 4, 8 and 16 weeks (Fig. 2F and G). Sixteen-week-old Myf5-fukutin-cKO mice showed more advanced pathological changes, such as fiber size variation and fibrosis (Fig. 2E). A few specimens showed milder phenotypic changes accompanied by increases in the normally glycosylated α-DG population (Supplementary Material, Fig. S2F). Overall, different phenotypes of the MCK-fukutin-cKO and Myf5-fukutin-cKO mice suggested a pathophysiological role of fukutin-dependent modification in MPCs.

Impaired viability of MPCs in Myf5-fukutin-cKO mice

To determine the impact of fukutin deficiency on MPC activity, we isolated SM/C-2.6(+) satellite cells from young (slightly affected) and adult (diseased) Myf5-fukutin-cKO muscles and then cultured them as MPCs (i.e. myoblasts) (28). The number of isolated SM/C-2.6(+) cells tended to be less in young fukutin-deficient muscles and was significantly reduced in adults compared with the litter controls (Fig. 3A). The proliferation activity of the isolated MPCs was slightly but significantly decreased in young and severely reduced in adult Myf5-fukutin-cKO muscles (Fig. 3B). The differentiation activity of fukutin-deficient myoblasts was significantly lower than that of the control mice (Fig. 3C). Quantification of the Pax7 immunofluorescence signal, a satellite cell marker, on skeletal muscle sections also suggested decreases in the number of satellite cells in adult Myf5-fukutin-cKO mice compared with control mice (Supplementary Material, Fig. S3A). We also examined the population of activated satellite cells by Pax7/MyoD double staining on the skeletal muscle sections from Myf5-fukutin-cKO mice. The results suggested that the number of active satellite cells was reduced in 16-week-old Myf5-fukutin-cKO mice compared with that in 8-week-old Myf5-fukutin-cKO mice (Supplementary Material, Fig. S3B). These data suggest that in addition to decreases in the number of satellite cells, the activation state of satellite cells is impaired in Myf5-cKO mice as the disease progresses.

We next examined *in vivo* regeneration capability of the Myf5-fuktuin-cKO muscles after cardiotoxin (CTX)-induced muscle degeneration. After 14 days of the CTX challenge in adult mice (~3 months old), we observed that the proportion of small myofibers was strikingly higher in Myf5-fukutin-cKO mice than in the controls (Fig. 3D and E). In some cases, the CTX-injected Myf5-fukutin-cKO muscles showed severe atrophic changes compared with the contralateral saline-injected ones (Supplementary Material, Fig. S3C). In younger (~4 weeks old) Myf5-fukutin-cKO mice, after 14 days of the CTX challenge, no obvious histological difference was noted compared with the controls (Supplementary Material, Fig. S3D); however, after 5 days of the CTX challenge, the proportion of smaller regenerating fibers (that are embryonic myosin-positive) was higher in Myf5-fukutin-cKO muscles than in the controls (Supplementary Material, Fig. S3E and F). These minor impairments in the regeneration of younger Myf5-fukutin-cKO skeletal muscles are consistent with the *in vitro* results. Overall, our data showed that fukutin-dependent

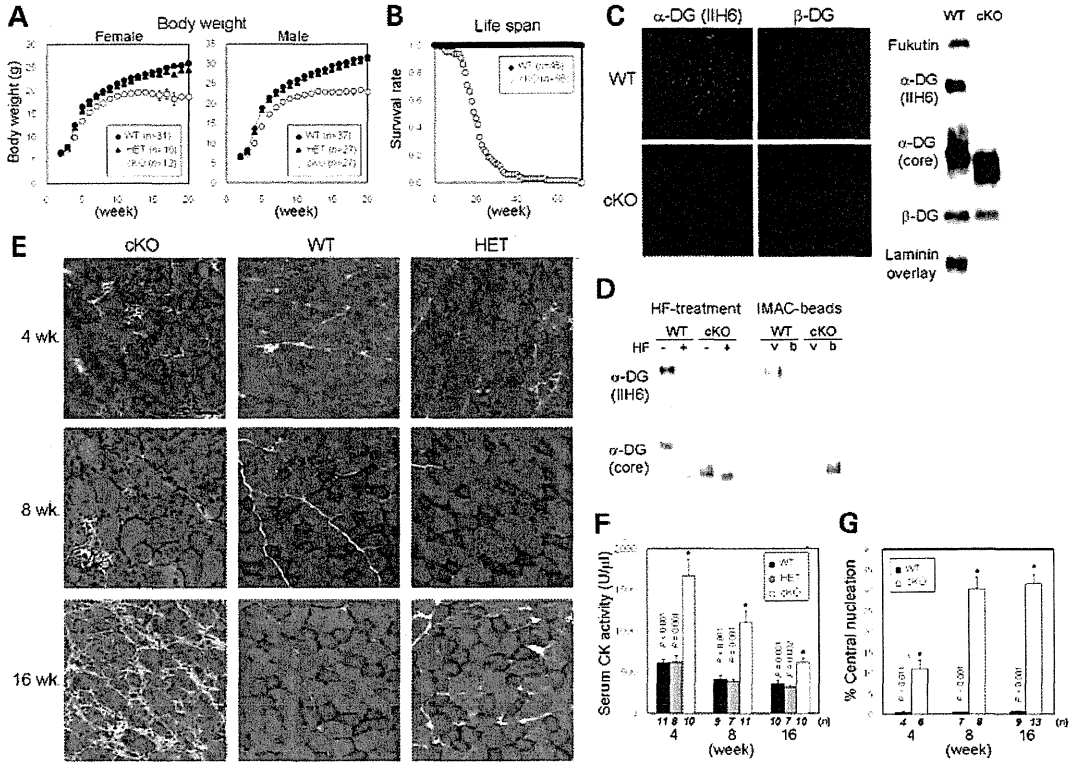

Figure 2. Pathological characterization of Myf5-fukutin-cKO mice. (**A**) Temporal changes in body weight. Data shown are mean ± SEM for each group (*n* is indicated in the graph). (**B**) Survival curve of Myf5-fukutin cKO mice. (**C**) Immunofluorescence and western blot analyses of fukutin expression and α-DG modification. Skeletal muscles of new born and 1-week-old Myf5-fukutin-cKO and control WT mice were used for immunofluorescence and western blotting, respectively. β-DG was used as a control. Laminin-binding activity of α-DG was examined by the laminin overlay assay. (**D**) Post-phosphoryl modification of α-DG from Myf5-fukutin-cKO and control WT skeletal muscles. The absence of post-phosphoryl modification was tested by HF treatment and IMAC-bead-binding assay. The void (v) and bound (b) fractions of the IMAC beads were analyzed by western blotting. (**E**) H&E staining of tibialis anterior muscles. Bar □50 μm. (**F**) Serum creatin kinase activity and (**G**) proportion of myofibers with centrally located nuclei. Data shown are mean ± SEM for each group (*n* is indicated in the graph). $^{*}P \leq 0.05$ for both cKO versus WT and cKO versus HET (F) and cKO versus WT (G) (Mann–Whitney *U* test; *P*-values are indicated in the graph).

modification plays important roles in maintaining MPC viability, and consequently, muscle regeneration capability, suggesting that these defects may contribute to the severe phenotype of dystroglycanopathy.

Amelioration of the severe pathology by limited fukutin rescue in myofibers

Our pathological analysis of the two distinct fukutin-cKO mice suggested that membrane fragility triggers disease manifestation and that impaired MPC viability is related to disease progression and severity of dystroglycanopathy. These findings indicate that a therapeutic strategy must involve prevention of myofiber membrane weakness and/or rescue of substantial loss and dysfunction of MPCs. In addition, dystroglycanopathy is usually diagnosed after disease manifestation, and thus, treatments should be effective even after disease progression. Since our data suggested that frequent cycles of myofiber degeneration/regeneration accelerate substantial and/or functional loss of MPC, we expected that protection from disease-triggering myofiber degeneration provides therapeutic effects even in mouse models with MPC defects. In this study, to prevent disease-causing myofiber degeneration, we examined whether rescue of fukutin expression that is limited in myofibers is therapeutically beneficial in Myf5-fukutin-cKO mice. Therefore, we constructed recombinant AAV9 (AAV, adeno-associated virus) vectors containing the mouse *fukutin* cDNA under the MCK promoter (AAV9-MCK-*fukutin*).

We first administered intramuscular injections of AAV9-MCK-*fukutin* to 1-week-old (i.e. before disease manifestation) or 8-week-old (i.e. after disease manifestation) Myf5-fukutin-cKO mice; then, we examined the therapeutic effects after 2 months. In both cases, fukutin protein expression was higher in the AAV-injected Myf5-fukutin-cKO muscles than in the control WT muscles (endogenous fukutin protein in muscle lysates is below detectable levels) (Fig. 4A and E). IIH6-positive α-DG was restored, indicating functional rescue of *fukutin* gene expression even in adult cases (Fig. 4A, B, E and F). Histological and quantitative analyses showed that gene transfer at 1 week prevented disease manifestation (Fig. 4C and D). When gene transfer was challenged in 8-week-old mice, H&E staining showed milder phenotype in AAV-treated Myf5-fukutin-cKO muscles than

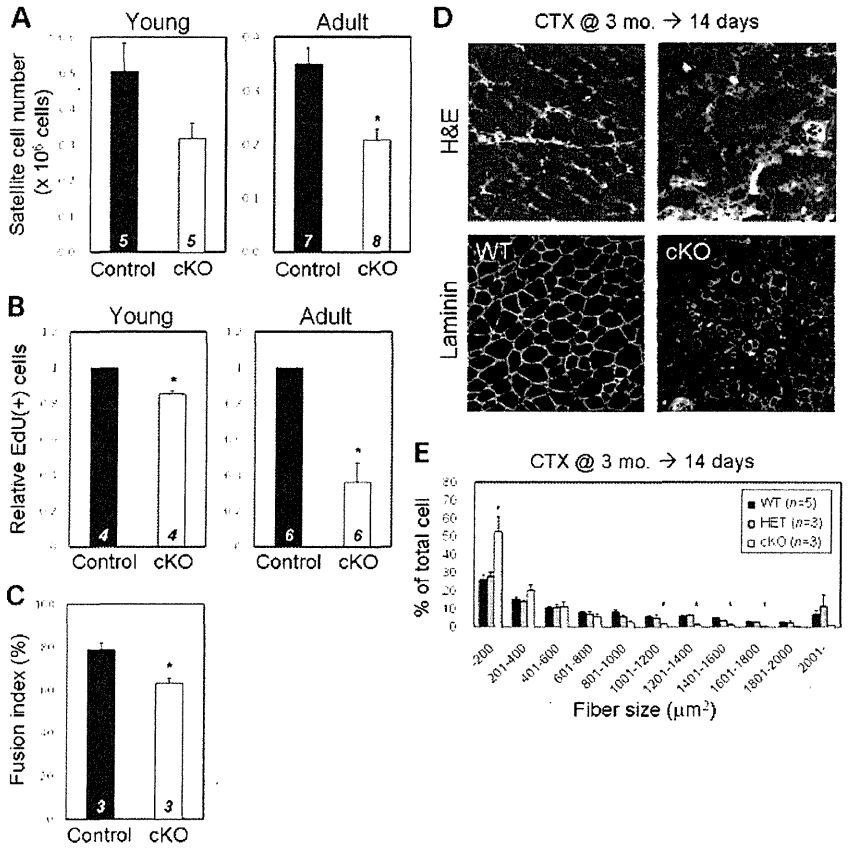

Figure 3. Impaired MPC activities and muscle regeneration in Myf5-fukutin-cKO mice. (**A**) The number of isolated satellite cells from young (2 weeks old) and adult (4 months old) Myf5-fukutin-cKO mice. P □0.117 for young, and P □0.005 for adult (Mann–Whitney U test). (**B**) Proliferation activity of the isolated MPCs. MPCs from young or adult Myf5-fukutin-cKO muscles were cultured for 2 days, and 5-ethynyl-2′-deoxyuridine-positive (EdU+) cells were counted. P □0.014 for young, and P □0.002 for adult (Mann–Whitney U test). (**C**) Differentiation activity of the isolated MPCs. MPCs from young Myf5-fukutin-cKO muscles were cultured in growth media for 2 days and then in differentiation media for 2 days. The cells were fixed, and multinucleated myotubes were counted. P □0.05 (Mann–Whitney U test). For (A)–(C), data shown are mean ± SEM for each group (n is indicated in the graph). $^*P \leq 0.05$ compared with litter controls (Mann–Whitney U test). (**D**) Regeneration after CTX-induced muscle degeneration. CTX was injected into the tibialis anterior muscles of 3-month-old Myf5-fukutin-cKO and control mice (WT and HET). After 14 days, the muscle sections were analyzed by H&E staining and immunofluorescence staining with laminin. (**E**) Quantitative analysis for myofiber size variation after the CTX challenge. Data shown are mean ± SEM for each group (n is indicated in the graph). $^*P \leq 0.05$ for both cKO versus WT and cKO versus HET (Mann–Whitney U test).

in non-treated ones (Fig. 4G). Quantitatively, connective tissue infiltration and prevalence of small fibers were significantly reduced (Fig. 4H and I), whereas a substantial number of myofibers with central nucleation was still present after the gene transfer (Fig. 4J).

Next, we examined systemic delivery of the *fukutin* gene via tail vein injection into 4-week-old Myf5-fukutin-cKO mice with early-stage muscular dystrophy, primarily because diagnosis occurs during this stage in humans. After 2 months of the injection, we confirmed fukutin protein expression and recovery of α-DG modification in the treated Myf5-fukutin-cKO mice (Fig. 5A and B). After gene transfer, body and muscle weight were restored (Fig. 5C and D), and grip strength was dramatically improved, indicating recovery of muscle physiological function (Fig. 5E). H&E staining (Fig. 5F) and quantitative analyses of connective tissue infiltration (Fig. 5G) and fiber size variation (Fig. 5H) showed amelioration of muscle pathology; however, there were still a few necrotic fibers and a substantial proportion of myofibers with centrally located nuclei (Fig. 5I). Similar therapeutic effects were also obtained in other muscles (Supplementary Material, Fig. S4). Our results show that limited recovery of fukutin expression in myofibers, even after disease progression, can successfully ameliorate the severe phenotype of Myf5-fukutin-cKO mice.

We also constructed recombinant AAV9 vectors containing the mouse *fukutin* cDNA under the CMV promoter (AAV9-CMV-*fukutin*), which is commonly used for driving the expression of transgenes in a wide range of cell types. Two months after tail-vein injection in 4-week-old Myf5-fukutin-cKO mice, we observed therapeutic effects similar to those observed in AAV9-MCK-*fukutin*-treated Myf5-fukutin-cKO mice (Supplementary Material, Fig. S5). There was no obvious difference in the efficiency for the recovery of IIH6 immunoreactivity (the proportion of IIH6-positive to laminin-positive fibers) between the cases of AAV9-MCK-*fukutin* (77.4 ± 3.8%, n □5) and AAV9-CMV-*fukutin* (74.8 ± 3.6%,

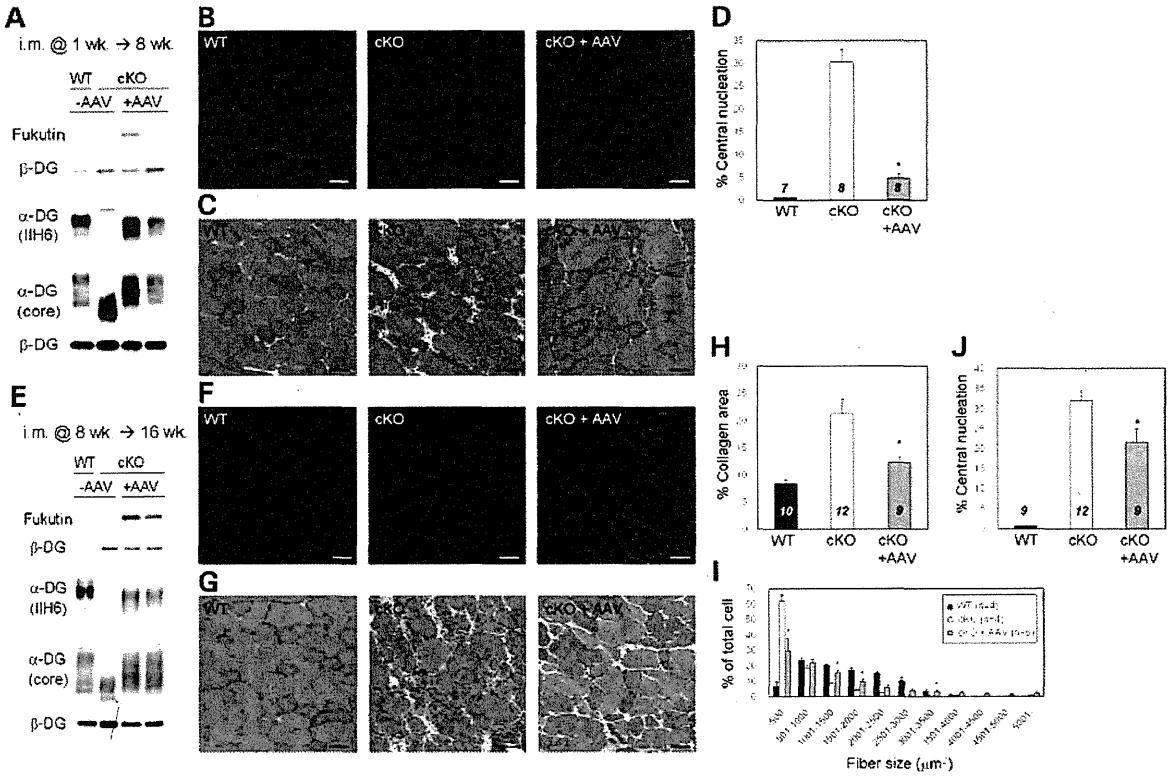

Figure 4. Gene transfer of *fukutin* via AAV9 intramuscular injection into Myf5-fukutin-cKO mice. AAV9-MCK-*fukutin* was administered to 1-week-old (**A**–**D**) and 8-week-old (**E**–**J**) Myf5-fukutin-cKO mice via intramuscular injection. Two months after the gene transfer, recovery of fukutin protein and α-DG glycosylation was confirmed by western blotting (A and E) and IIH6-immunofluorescence staining (B and F) (bar □50 μm). For fukutin protein expression and α-DG modification, total lysate and wheat germ agglutinin-enriched fractions, respectively, were subjected to western blotting. In both cases, β-DG was used as a loading control. Western blotting results for two AAV-treated mice are shown. Therapeutic effects were quantitatively evaluated in terms of the proportion of myofibers with centrally located nuclei (D; P □0.001, J; P □0.023), connective tissue infiltration (H; P □0.016) and fiber size variation (I; $^*P \leq 0.05$). Data shown are mean ± SEM for each group (n is indicated in the graph). $^*P \leq 0.05$ compared with non-treated cKO mice (Mann–Whitney U test).

n □5). In addition, the population of myofibers with centrally located nuclei was significantly improved (Supplementary Material, Fig. S5I). We also examined the effects of intraperitoneal injections of AAV9-CMV-*fukutin* in 1-week-old Myf5-fukutin-cKO mice. Two months after the injections, we observed partial recovery of α-DG glycosylation and amelioration of the pathology compared with that observed in non-treated Myf5-fukutin-cKO mice (Supplementary Material, Fig. S6A–D).

The predominant mutation in FCMD is a retrotransposon insertion (4). We previously generated a transgenic knock-in mouse model carrying this insertion (29). The knock-in Hp/− mice represent compound heterozygotes for the insertion and a nonsense *fukutin* mutation. Although Hp/− mice show abnormal glycosylation of α-DG, a small amount of intact α-DG is also present; this prevents muscular dystrophy (29). We administered intraperitoneal injections of AAV9-CMV-*fukutin* to 1-week-old Hp/− mice and examined α-DG glycosylation status after 16 and 48 weeks. We detected increased levels of fukutin expression and IIH6-positive α-DG in the AAV-treated Hp/− skeletal muscles even 48 weeks after the gene transfer (Supplementary Material, Fig. S6E). These data suggest that the transferred *fukutin* gene persists in correcting abnormal glycosylation of α-DG for a considerable length of time.

DISCUSSION

In this study, we developed and analyzed two distinct *fukutin* cKO mice to understand the pathogenesis and to establish a therapeutic strategy for dystroglycanopathy. Our data showed that MPC-selective Myf5-fukutin-cKO mice exhibited more severe phenotypes of muscular dystrophy than myofiber-selective MCK-fukutin-cKO mice. Very recently, Campbell and colleagues also generated *fukutin* cKO mice, using Myf5-Cre and MCK-Cre mice (30). Pathological analysis of our Myf5-fukutin-cKO and MCK-fukutin-cKO mice showed results that were mostly consistent with those reported by Campbell and colleagues: increased serum CK levels in both cKO lines; milder phenotypes of MCK-fukutin-cKO than Myf5-fukutin-cKO; and decreases in grip strength, body mass and longevity of Myf5-fukutin-cKO mice. Our study includes further detailed histopathological characterization of the disease onset and progression in both lines. More importantly, our present study clarifies features of dystroglycanopathy that

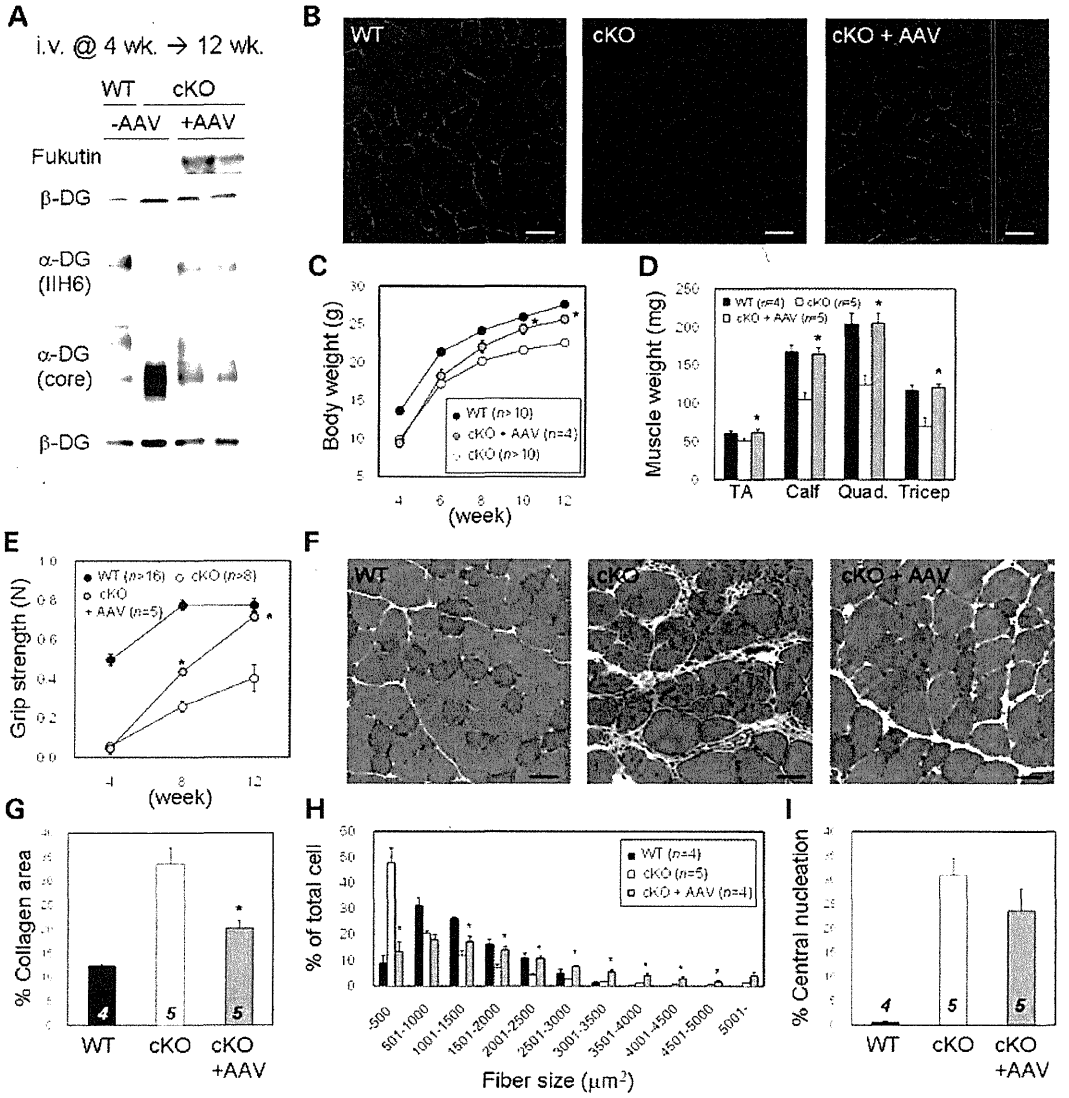

Figure 5. Systemic gene transfer of *fukutin* into Myf5-fukutin-cKO mice. AAV9-MCK-*fukutin* was administered to 4-week-old Myf5-fukutin-cKO mice via tail vein injection. Two months after the gene transfer, the skeletal muscles were analyzed and compared with non-treated Myf5-fukutin-cKO muscles. Recovery of fukutin protein and α-DG modification was confirmed by western blotting (**A**) and immunofluorescence (**B**) (bar □50 μm). For fukutin protein expression and α-DG modification, total lysate and wheat germ agglutinin-enriched fractions, respectively, were subjected to western blotting. In both cases, β-DG was used as a loading control. Therapeutic effects were evaluated by body weight change (**C**; P □0.016 and 0.01 for 10 and 12 weeks, respectively) and muscle weight change (**D**; P □0.047 for tibialis anterior, and 0.014 for other muscles), grip strength (**E**; P □0.007 and 0.003 for 8 and 12 weeks, respectively), H&E staining (**F**) (bar □50 μm), connective tissue infiltration estimated by quantification of collagen I immunoreactive areas (**G**; P □0.028), fiber size variation (**H**; $^*P \leq 0.05$) and central nucleation (**I**). Data from the tibialis anterior muscle are shown (F–I). Histopathology (F) and quantitative analyses (G and H) indicate amelioration of disease severity after the gene transfer. Data shown are mean ± SEM for each group (n is indicated in the graph). $^*P \leq 0.05$ compared with the non-treated cKO mice (Mann–Whitney U test). TA, tibialis anterior; Quad., quadricep.

enhance our understanding of its pathogenesis—specifically, the trigger initiating disease pathogenesis and the biological mechanism underlying the severe phenotype.

Our study provides direct evidence using presymptomatic fukutin-deficient mice that myofiber membrane fragility triggers disease manifestation. Although histological data in both studies suggested regeneration delay or impairment in Myf5-fukutin-cKO skeletal muscles, our study provides the first direct evidence for impaired MPC activity and viability using the isolated myoblast culture system. We observed that the proliferation and differentiation activities of the isolated MPCs from little-affected young Myf5-fukutin-cKO muscles were decreased, which may suggest that fukutin-dependent modification of α-DG plays a role in MPCs. Furthermore, our data showed that MPC proliferation and muscle regeneration deteriorate more severely as the disease progresses. The mechanisms underlying the decreases in the number of isolated satellite cells and MPC proliferation are

currently unknown. It has been suggested that satellite cells express properly glycosylated α-DG (31) and that myoblasts/MPCs also express properly glycosylated α-DG although its signals are relatively weak compared with those of myotubes (32,33). The basement membrane of skeletal muscle contains DG ligands, laminins and perlecan. It is well established that interactions between the extracellular matrix and cell-surface receptors are involved in cell survival signaling (34). Since it has been proposed that DG-ligand interactions are also involved in cellular signaling mechanisms such as survival and apoptosis pathways (35,36), it is possible that loss of α-DG glycosylation may affect survival signaling regulated by α-DG-basement membrane interaction. In addition, since the Myf5-fukutin-cKO myofibers showed an earlier reduction of fukutin compared with those of MCK-fukutin-cKO, there is a possibility that earlier loss of α-DG glycosylation in myofibers affects disease progression and severity. For example, the absence of α-DG glycosylation during postnatal/juvenile muscle growth and development may have a high impact on muscle degeneration and/or dystrophic pathology in later stages.

As for other muscular dystrophy models with defects in the dystrophin–glycoprotein complex, impaired muscle regeneration has also been reported in *MORE-DG null* mice, in which the DG gene (*Dag1*) is ablated in all cells in the embryo (31), and in older (>1 year) dystrophin-deficient mdx and sarcoglycan-deficient mice (31). The regeneration defects in our Myf5-fukutin-cKO mice appeared at a relatively young age (~3 months), but at this age, Myf5-fukutin-cKO mice already show severe dystrophic pathology. The pathological environment may interfere with efficient muscle regeneration, resulting in decreased regeneration activity as the disease progresses (37). A very recent study also suggested that alterations to the basal lamina microenvironment perturb regeneration potential in dystroglycanopathy (38). Moreover, our data suggest that multiple cycles of degeneration/regeneration may also affect MPC viability, which is consistent with a previous study showing that the progressive exhaustion of functional muscle satellite cells is associated with severe dystrophic phenotype (39). It appears that these disease environments and impaired MPC viability caused by loss of fukutin-dependent modification additively deteriorate regeneration activity, eventually leading to severe and rapid progressive pathology. Together, we conclude that defects in MPC activity contribute to the severe pathology of dystroglycanopathy and propose that dystroglycanopathy is a regeneration-defective disorder.

We observed that some muscle specimens from 16-week-old Myf5-fukutin-cKO mice showed mild phenotype, which was consequently supported by the presence of functionally glycosylated α-DG. Beedle *et al.* (30) also reported that fukutin deletion resulted in moderate to severe muscular dystrophy using Myf5-Cre mice. Because phenotypic variation in our Myf5-fukutin-cKO colony was rarely seen before 12 weeks of age, the variation may be secondary to disease progression. The less phenotypic variation in our colonies could also be due to the number of backcross on C57BL/6 (backcross: more than seven). We speculate that during frequent cycles of muscle degeneration/regeneration, Myf5-independent or less-expressed myogenic cells (40) may be activated and differentiated into myofibers in which the *fukutin* gene escaped Cre-mediated recombination.

Many cases of dystroglycanopathy show the most severe skeletal muscle phenotype, and the severe/typical dystroglycanopathy patients end their short lives without ever standing or walking. Although an increasing number of patients are being diagnosed with dystroglycanopathy worldwide, there have been no therapeutic studies on dystroglycanopathy models after the disease progresses. In this study, for the first time, we succeeded in ameliorating the disease severity in dystroglycanopathy mouse models based on the pathomechanism. It is of importance that limited rescue of fukutin protein in myofibers of Myf5-fukutin-cKO muscles, which have MPC defects, ameliorated the severe phenotype. These data suggest that even after functional and/or substantial loss of MPC occurs, prevention of disease-causing defects in myofibers is a probable therapeutic strategy for muscular dystrophy. Moreover, it is noteworthy that therapeutic effects of the exogenous *fukutin* gene were achieved with relatively lower AAV titers than those used in other gene therapies for structural proteins such as dystrophin and sarcoglycans (41–43). Our results showed that titers that were ~2 orders of magnitude less than those required in previous studies were sufficient to produce a therapeutic effect in Myf5-fukutin-cKO mice. This is consistent with our previous study, which suggested that only a little amount of fukutin is necessary to prevent muscular dystrophy (29). Most dystroglycanopathy genes are identified as glycosyltransferases (11,12,15) or hypothesized to have enzyme-like properties, suggesting that a small amount of exogenous gene would be sufficient for producing therapeutic effects. A small dose of AAV vectors could lower the chances of adverse effects such as immune responses in human (44). In addition, the cDNA sizes of fukutin as well as other dystroglycanopathy genes are suitable for AAV vectors. Taken together, we propose that gene transfer is a promising therapeutic strategy for the amelioration of the severe skeletal muscle pathology of dystroglycanopathy. Human dystroglycanopathy is frequently accompanied by brain and, often, cardiac disorders (1,45). The efficacy of AAV delivery to these affected tissues, timing of administration and therapeutic effects in other fukutin-cKO models should be examined in the future. Although therapeutic interventions that rescue the developmental defects of dystroglycanopathy (such as anomalies in brain structure) are difficult at present, amelioration of the muscle phenotype would be highly beneficial to patients and their families. For example, such treatment might improve patients' physical abilities and postpone the need for respiratory interventions until much later in the course of the disease. Increased physical activity could positively influence both mental development and social interactions. Overall, this study may facilitate future clinical translational research in the field of dystroglycanopathy treatment.

MATERIALS AND METHODS

Generation of fukutin cKO mice

Construction of the targeted allele, establishment of targeted embryonic stem (ES) cells and generation of the chimera

and F1 mice were carried out by Unitech Co. (Kashiwa, Japan). Briefly, exon 2 of mouse *fukutin* was flanked by two loxP sequences (Supplementary Material, Fig. S1A). An Flp recognition target-flanked neo-cassette was inserted upstream of exon 2. The targeting vector was electroporated into C57BL/6 mouse ES cells. Positive clones were selected, and homologous recombination was confirmed by Southern blotting (Supplementary Material, Fig. S1B). The targeted ES cells were injected into blastocysts (BALB/c), and then, chimera mice were bred with C57BL/6 mice to generate founder mice. The founder mice were crossed with the FLPe transgenic mice, producing heterozygous flox mice without the neo-cassette ($fukutin^{lox/+}$). The heterozygous flox mice were intercrossed to obtain homozygous flox mice ($fukutin^{lox/lox}$).

MCK-Cre mice (22) [$MCK\text{-}Cre^{Tg}(+)$, backcrossed for at least 10 generations to C57BL/6] and Myf5-Cre knock-in mice (23) [$Myf5\text{-}Cre^{KI}(+)$] were obtained from The Jackson Laboratory. Myf5-Cre mice were backcrossed for more than six generations to C57BL/6 before crossing with $fukutin^{lox/lox}$ mice. The heterozygous $fukutin^{lox/+}$ carrying MCK-Cre [$fukutin^{lox/+}$:$MCK\text{-}Cre^{Tg}(+)$] or Myf5-Cre [$fukutin^{lox/+}$:$Myf5\text{-}Cre^{KI}(+)$] were then bred with $fukutin^{lox/lox}$ mice to obtain cKO mice. Using this breeding strategy, we obtained the following four genotypes (Supplementary Material, Fig. S1C): for MCK-fukutin-cKO line—[$fukutin^{lox/lox}$:$MCK\text{-}Cre^{Tg}(-)$] (used as WT control), [$fukutin^{lox/lox}$:$MCK\text{-}Cre^{Tg}(+)$] (used as cKO), [$fukutin^{lox/+}$:$MCK\text{-}Cre^{Tg}(+)$] (used as heterozygous control, HET) and [$fukutin^{lox/+}$:$MCK\text{-}Cre^{Tg}(-)$]; and for the Myf5-fukutin-cKO line—[$fukutin^{lox/lox}$:$Myf5\text{-}Cre^{KI}(-)$] (used as WT), [$fukutin^{lox/lox}$:$Myf5\text{-}Cre^{KI}(+)$] (used as cKO), [$fukutin^{lox/+}$:$Myf5\text{-}Cre^{KI}(+)$] (used as HET) and [$fukutin^{lox/+}$:$Myf5\text{-}Cre^{KI}(-)$]. Alternatively, we crossed cKO mice with $fukutin^{lox/lox}$ mice to obtain two genotypes: WT and cKO (Supplementary Material, Fig. S1C). Genotyping was performed using PCR (Supplementary Material, Fig. S1D). Primer sequences and PCR conditions are available on request. Mice were maintained in accordance with the animal care guidelines of Unitech Co. Ltd., Osaka University and Kobe University.

Antibodies

Antibodies used in western blots and immunofluorescence were as follows: mouse monoclonal antibody 8D5 against β-DG (Novacastra); mouse monoclonal antibody IIH6 against glycosylated α-DG (Millipore); goat polyclonal antibody against the C-terminal domain of the α-DG polypeptide (AP-074G-C) (29); goat polyclonal anti-fukutin antibody (106G2) and rabbit polyclonal anti-fukutin antibody (RY213) (5); rat anti-laminin antibody 4H8-2 (Alexis Biochemicals); rabbit polyclonal anti-collagen I antibody (AbD Serotec); and mouse monoclonal anti-embryonic myosin antibody (The Developmental Studies Hybridoma Bank, University of Iowa). A rat monoclonal antibody against the α-DG core protein (3D7-7) was generated using the recombinant α-DG-Fc fusion protein (46); hybridoma clones were selected for reactivity to the C-terminal domain of the α-DG polypeptide. To reduce high background staining of IIH6 in severely affected skeletal muscle sections, commercial IIH6 was labeled with biotin. The IIH6-IgM fractions were prepared from ascites, using protein L-beads (Pierce) and then biotinylated (EZ-Link Micro Sulfo-NHS-Biotinylation Kit; Pierce) according to the manufacturer's instructions.

Preparation of fukutin and DG

Endogenous fukutin was enriched by immunoprecipitation using polyclonal goat anti-fukutin antibody (106G2) from the skeletal muscle lysates. The immunoprecipitated materials were subjected to western blotting using polyclonal rabbit anti-fukutin antibody (RY213). DG from solubilized skeletal muscle was enriched with wheat germ agglutinin-agarose beads (Vector Laboratories) as previously described (29).

Histological and immunofluorescence analyses

For histological and immunofluorescence staining, cryosections (7 μm thick) were prepared. For H&E staining, sections were stained for 2 min in hematoxylin, 1 min in eosin, and then dehydrated with ethanol and xylene. The slides are washed with 0.5% glacial acetic acid, dehydrated and then mounted. For immunofluorescence analysis, sections were treated with cold ethanol/acetic acid (1:1) for 1 min, blocked with 5% goat serum in MOM mouse Ig blocking reagent (Vector Laboratories) at room temperature for 1 h, and then incubated overnight with primary antibodies diluted in MOM diluent (Vector Laboratories) at 4°C. The slides were washed with phosphate-buffered saline (PBS) and incubated with Alexa Fluor 488-conjugated or Alexa Fluor 555-conjugated secondary antibodies (Molecular Probes) at room temperature for 30 min. Sections were observed by fluorescence microscopy (Leica DMR, Leica Microsystems and BZ9000, Keyence). Quantification of the number of Pax7-positive cells and the population of Pax7/MyoD-double-positive cells was performed as previously described (47).

Quantitative and statistical analysis

For quantitative evaluation of muscle pathology, the proportion of myofibers with centrally located nuclei in at least 1000 fibers for each individual was counted. For the evaluation of connective tissue infiltration, the immunofluorescence signal of collagen I was quantitatively measured using the ImageJ software. For the assessment of myofiber size variation, areas of individual myofibers on transverse sections were measured using the ImageJ software. Data represent means with SEM, and P-values ≤ 0.05 were considered statistically significant (Mann–Whitney U test).

Preparation and culture of MPCs

Mononuclear cells from uninjured limb muscles were prepared using 0.2% collagenase type II (Worthington Biochemical) as previously described (28,48). Approximately $3-5 \times 10^6$ or $3-9 \times 10^6$ mononuclear cells from young mice (2-week-old) or adult mice (4-month-old), respectively, were subjected to MPC isolation experiments. Mononuclear cells derived from the skeletal muscles were stained with FITC-conjugated anti-CD31 (Pecam1, Mouse Genome Informatics), anti-CD45

(Ptprc, Mouse Genome Informatics), phycoerythrin-conjugated anti-Sca1 (Ly6a, Mouse Genome Informatics) and biotinylated SM/C-2.6 antibodies (28). Cells were then incubated with 1:400 streptavidin–allophycocyanin (BD Biosciences) on ice for 30 min and resuspended in PBS containing 2% fetal calf serum (FCS) and 2 μg/ml propidium iodide (PI). Cell sorting was performed using an FACS Aria II flow cytometer (BD Immunocytometry Systems). Debris and dead cells were excluded by forward scatter, side scatter and PI gating. Data were collected using the FACSDiva software (BD Biosciences). Myogenic cells from the regenerating muscles were also highly enriched in the SM/C-2.6(+) CD31(−) CD45(−) Sca1(−) cell fraction.

Freshly isolated myogenic cells were cultured in a growth medium of high-glucose Dulbecco's modified Eagle's medium (DMEM-HG; Sigma-Aldrich) containing 20% FCS, 2.5 ng/ml basic fibroblast growth factor (FGF2; PeproTech) and penicillin (100 U/ml)–streptomycin (100 μg/ml) (Gibco BRL) on culture dishes coated with Matrigel (BD Biosciences). Differentiation was induced in a differentiation medium containing DMEM-HG, 5% horse serum and penicillin–streptomycin for 3–4 days. Quantitative analysis for cell proliferation was performed as described previously (47). Fusion index was estimated as the ratio of nuclei in the myotubes to all the nuclei in more than four independent microscopy fields.

CTX experiments

CTX (30 μM; purified from the venom of the snake *Naja nigricollis*; Latoxan) was injected intramuscularly (for young mice, 30 μl to the tibialis anterior and 70 μl to the calf; for adult mice, 50 μl to the tibialis anterior and 100 μl to the calf). Mock injections used only saline solution. The injected muscles were examined 5 or 14 days after the injection. Five days after the injection, areas of individual embryonic myosin-positive fibers were measured (>300 fibers randomly chosen from 5–10 regions per toxin-challenged muscle) in each genotype. Fourteen days after the injection, fiber size variation was quantitatively evaluated by measuring individual laminin-positive fibers (>300 fibers) in each genotype.

AAV gene transfer

To generate *fukutin*-encoding AAV9 vector, the complete open reading frame of mouse *fukutin* gene was cloned into the pAAV-IRES-hrGFP vector (49). The recombinant *fukutin*-encoding AAV9 vector was produced as described previously (49). AAV vectors were injected intramuscularly into the calf and tibialis anterior (at 1 week to the tibialis anterior, $0.8–1.6 \times 10^9$ vector genome in saline solution; at 1 week to the calf or at 8 weeks to the tibialis anterior, $2–4 \times 10^9$ vector genome; and at 8 weeks to the calf, $4–8 \times 10^9$ vector genome). For tail vein injections and intraperitoneal injections, $\sim 2 \times 10^{10}$ and $\sim 1 \times 10^{10}$ vector genome was used, respectively.

Miscellaneous

For western blotting, the proteins were separated using 4–15% linear gradient SDS–PAGE (Bio-Rad). Gels were transferred to polyvinylidene fluoride membrane (Millipore). Blots were developed by horseradish peroxidase-enhanced chemiluminescence (Supersignal West Pico, Pierce; or ECL Plus, GE Healthcare). Laminin-binding activity was determined by the laminin overlay assay as described previously (29). Serum CK activity was measured using the CPK kit (WAKO). For Evans blue dye uptake, Evans blue dye (10 mg/ml in saline) was intraperitoneally injected (100 μl/10 g of body weight). After 5 h, the mice were made to exercise on a downhill (15°) treadmill for 60 min (MK-680S, Muromachi Kikai). Twenty-four hours after the exercise, frozen tissue samples were prepared. Serum was prepared before 24 h and after 2 h of the exercise. Grip strength was measured for 10 consecutive trials for each mouse, using a strength meter (Ohara Ika Sangyo Co. Ltd, Tokyo), and 20% of the top and the bottom values were excluded to obtain the mean value.

SUPPLEMENTARY MATERIAL

Supplementary Material is available at *HMG* online.

ACKNOWLEDGEMENTS

We would like to thank the past and present members of T.T.'s laboratory for fruitful discussions and scientific contributions. We also thank Hiromi Hayashita-Kinoh for providing technical support.

Conflict of Interest statement. None declared.

FUNDING

This work was supported by the Ministry of Health, Labor and Welfare of Japan [Intramural Research Grant for Neurological and Psychiatric Disorders of National Center of Neurology and Psychiatry (23B-5)], the Ministry of Education, Culture, Sports, Science and Technology of Japan [a Grant-in-Aid for Scientific Research (A) 23249049 to T.T., a Grant-in-Aid for Young Scientists (A) 24687017 to M.K. and a Grant-in-Aid for Scientific Research on Innovative Areas (No. 23110002, Deciphering Sugar Chain-based Signals Regulating Integrative Neuronal Functions) 24110508 to M.K.], a Senri Life Science Foundation grant to M.K., a Takeda Science Foundation grant to M.K. and a Naito Foundation grant to M.K.

REFERENCES

1. Godfrey, C., Foley, A.R., Clement, E. and Muntoni, F. (2011) Dystroglycanopathies: coming into focus. *Curr. Opin. Genet. Dev.*, **21**, 278–285.
2. Hayashi, Y.K., Ogawa, M., Tagawa, K., Noguchi, S., Ishihara, T., Nonaka, I. and Arahata, K. (2001) Selective deficiency of alpha-dystroglycan in Fukuyama-type congenital muscular dystrophy. *Neurology*, **57**, 115–121.
3. Michele, D.E., Barresi, R., Kanagawa, M., Saito, F., Cohn, R.D., Satz, J.S., Dollar, J., Nishino, I., Kelley, R.I., Somer, H. *et al.* (2002) Post-translational disruption of dystroglycan-ligand interactions in congenital muscular dystrophies. *Nature*, **418**, 417–422.
4. Kobayashi, K., Nakahori, Y., Miyake, M., Matsumura, K., Kondo-Iida, E., Nomura, Y., Segawa, M., Yoshioka, M., Saito, K., Osawa, M. *et al.* (1998) An ancient retrotransposal insertion causes Fukuyama-type congenital muscular dystrophy. *Nature*, **394**, 388–392.

5. Taniguchi-Ikeda, M., Kobayashi, K., Kanagawa, M., Yu, C.C., Mori, K., Oda, T., Kuga, A., Kurahashi, H., Akman, H.O., DiMauro, S. *et al.* (2011) Pathogenic exon-trapping by SVA retrotransposon and rescue in Fukuyama muscular dystrophy. *Nature*, **478**, 127–131.
6. Fukuyama, Y., Osawa, M. and Suzuki, H. (1981) Congenital progressive muscular dystrophy of the Fukuyama type-clinical, genetic and pathological considerations. *Brain Dev.*, **3**, 1–29.
7. Godfrey, C., Clement, E., Mein, R., Brockington, M., Smith, J., Talim, B., Straub, V., Robb, S., Quinlivan, R., Feng, L. *et al.* (2007) Refining genotype phenotype correlations in muscular dystrophies with defective glycosylation of dystroglycan. *Brain*, **130**, 2725–2735.
8. Tachikawa, M., Kanagawa, M., Yu, C.C., Kobayashi, K. and Toda, T. (2012) Mislocalization of fukutin protein by disease-causing missense mutations can be rescued with treatments directed at folding amelioration. *J. Biol. Chem.*, **287**, 8398–8406.
9. Wells, L. (2013) The O-mannosylation pathway: glycosyltransferases and proteins implicated in congenital muscular dystrophy. *J. Biol. Chem.*, **288**, 6930–6935.
10. Buysse, K., Riemersma, M., Powell, G., van Reeuwijk, J., Chitayat, D., Roscioli, T., Kamsteeg, E.J., van den Elzen, C., van Beusekom, E., Blaser, S. *et al.* (2013) Missense mutations in β-1,3-*N*-acetylglucosaminyltransferase 1 (B3GNT1) cause Walker-Warburg syndrome. *Hum. Mol. Genet.*, **22**, 1746–1754.
11. Manya, H., Chiba, A., Yoshida, A., Wang, X., Chiba, Y., Jigami, Y., Margolis, R.U. and Endo, T. (2004) Demonstration of mammalian protein *O*-mannosyltransferase activity: coexpression of POMT1 and POMT2 required for enzymatic activity. *Proc. Natl Acad. Sci. USA*, **101**, 500–505.
12. Yoshida, A., Kobayashi, K., Manya, H., Taniguchi, K., Kano, H., Mizuno, M., Inazu, T., Mitsuhashi, H., Takahashi, S., Takeuchi, M. *et al.* (2001) Muscular dystrophy and neuronal migration disorder caused by mutations in a glycosyltransferase, POMGnT1. *Dev. Cell*, **1**, 717–724.
13. Yoshida-Moriguchi, T., Yu, L., Stalnaker, S.H., Davis, S., Kunz, S., Madson, M., Oldstone, M.B., Schachter, H., Wells, L. and Campbell, K.P. (2010) *O*-mannosyl phosphorylation of alpha-dystroglycan is required for laminin binding. *Science*, **327**, 88–92.
14. Kuga, A., Kanagawa, M., Sudo, A., Chan, Y.M., Tajiri, M., Manya, H., Kikkawa, Y., Nomizu, M., Kobayashi, K., Endo, T. *et al.* (2012) Absence of post-phosphoryl modification in dystroglycanopathy mouse models and wild-type tissues expressing non-laminin binding form of α-dystroglycan. *J. Biol. Chem.*, **287**, 9560–9567.
15. Inamori, K., Yoshida-Moriguchi, T., Hara, Y., Anderson, M.E., Yu, L. and Campbell, K.P. (2012) Dystroglycan function requires xylosyl- and glucuronyltransferase activities of LARGE. *Science*, **335**, 93–96.
16. Ibraghimov-Beskrovnaya, O., Ervasti, J.M., Leveille, C.J., Slaughter, C.A., Sernett, S.W. and Campbell, K.P. (1992) Primary structure of dystrophin-associated glycoproteins linking dystrophin to the extracellular matrix. *Nature*, **355**, 696–702.
17. Barresi, R. and Campbell, K.P. (2006) Dystroglycan: from biosynthesis to pathogenesis of human disease. *J. Cell Sci.*, **119**, 199–207.
18. Taniguchi, M., Kurahashi, H., Noguchi, S., Fukudome, T., Okinaga, T., Tsukahara, T., Tajima, Y., Ozono, K., Nishino, I., Nonaka, I. and Toda, T. (2006) Aberrant neuromuscular junctions and delayed terminal muscle fiber maturation in alpha-dystroglycanopathies. *Hum. Mol. Genet.*, **15**, 1279–1289.
19. Hara, Y., Balci-Hayta, B., Yoshida-Moriguchi, T., Kanagawa, M., Beltrán-Valero de Bernabé, D., Gündeşli, H., Willer, T., Satz, J.S., Crawford, R.W., Burden, S.J. *et al.* (2011) A dystroglycan mutation associated with limb-girdle muscular dystrophy. *N. Engl. J. Med.*, **364**, 939–946.
20. Roscioli, T., Kamsteeg, E.J., Buysse, K., Maystadt, I., van Reeuwijk, J., van den Elzen, C., van Beusekom, E., Riemersma, M., Pfundt, R., Vissers, L.E. *et al.* (2012) Mutations in ISPD cause Walker-Warburg syndrome and defective glycosylation of α-dystroglycan. *Nat. Genet.*, **44**, 581–585.
21. Willer, T., Lee, H., Lommel, M., Yoshida-Moriguchi, T., de Bernabe, D.B., Venzke, D., Cirak, S., Schachter, H., Vajsar, J., Voit, T. *et al.* (2012) ISPD loss-of-function mutations disrupt dystroglycan O-mannosylation and cause Walker-Warburg syndrome. *Nat. Genet.*, **44**, 575–580.
22. Brüning, J.C., Michael, M.D., Winnay, J.N., Hayashi, T., Hörsch, D., Accili, D., Goodyear, L.J. and Kahn, C.R. (1998) A muscle-specific insulin receptor knockout exhibits features of the metabolic syndrome of NIDDM without altering glucose tolerance. *Mol. Cell*, **2**, 559–569.
23. Tallquist, M.D., Weismann, K.E., Hellström, M. and Soriano, P. (2000) Early myotome specification regulates PDGFA expression and axial skeleton development. *Development*, **127**, 5059–5070.
24. Lyons, G.E., Mühlebach, S., Moser, A., Masood, R., Paterson, B.M., Buckingham, M.E. and Perriard, J.C. (1991) Developmental regulation of creatine kinase gene expression by myogenic factors in embryonic mouse and chick skeletal muscle. *Development*, **113**, 1017–1029.
25. Trask, R.V. and Billadello, J.J. (1990) Tissue-specific distribution and developmental regulation of M and B creatine kinase mRNAs. *Biochim. Biophys. Acta*, **1049**, 182–188.
26. Vilquin, J.T., Brussee, V., Asselin, I., Kinoshita, I., Gingras, M. and Tremblay, J.P. (1998) Evidence of mdx mouse skeletal muscle fragility in vivo by eccentric running exercise. *Muscle Nerve*, **21**, 567–576.
27. Durbeej, M., Sawatzki, S.M., Barresi, R., Schmainda, K.M., Allamand, V., Michele, D.E. and Campbell, K.P. (2003) Gene transfer establishes primacy of striated vs. smooth muscle sarcoglycan complex in limb-girdle muscular dystrophy. *Proc. Natl Acad. Sci. USA*, **100**, 8910–8915.
28. Fukada, S., Higuchi, S., Segawa, M., Koda, K., Yamamoto, Y., Tsujikawa, K., Kohama, Y., Uezumi, A., Imamura, M., Miyagoe-Suzuki, Y. *et al.* (2004) Purification and cell-surface marker characterization of quiescent satellite cells from murine skeletal muscle by a novel monoclonal antibody. *Exp. Cell Res.*, **296**, 245–255.
29. Kanagawa, M., Nishimoto, A., Chiyonobu, T., Takeda, S., Miyagoe-Suzuki, Y., Wang, F., Fujikake, N., Taniguchi, M., Lu, Z., Tachikawa, M. *et al.* (2009) Residual laminin-binding activity and enhanced dystroglycan glycosylation by LARGE in novel model mice to dystroglycanopathy. *Hum. Mol. Genet.*, **18**, 621–631.
30. Beedle, A.M., Turner, A.J., Saito, Y., Lueck, J.D., Foltz, S.J., Fortunato, M.J., Nienaber, P.M. and Campbell, K.P. (2012) Mouse fukutin deletion impairs dystroglycan processing and recapitulates muscular dystrophy. *J. Clin. Invest.*, **122**, 3330–3342.
31. Cohn, R.D., Henry, M.D., Michele, D.E., Barresi, R., Saito, F., Moore, S.A., Flanagan, J.D., Skwarchuk, M.W., Robbins, M.E., Mendell, J.R., Williamson, R.A. and Campbell, K.P. (2002) Disruption of DAG1 in differentiated skeletal muscle reveals a role for dystroglycan in muscle regeneration. *Cell*, **110**, 639–648.
32. Barresi, R., Michele, D.E., Kanagawa, M., Harper, H.A., Dovico, S.A., Satz, J.S., Moore, S.A., Zhang, W., Schachter, H., Dumanski, J.P. *et al.* (2004) LARGE can functionally bypass alpha-dystroglycan glycosylation defects in distinct congenital muscular dystrophies. *Nat. Med.*, **10**, 696–703.
33. Hara, Y., Kanagawa, M., Kunz, S., Yoshida-Moriguchi, T., Satz, J.S., Kobayashi, Y.M., Zhu, Z., Burden, S.J., Oldstone, M.B. and Campbell, K.P. (2011) Like-acetylglucosaminyltransferase (LARGE)-dependent modification of dystroglycan at Thr-317/319 is required for laminin binding and arenavirus infection. *Proc. Natl Acad. Sci. USA*, **108**, 17426–17431.
34. Gilmore, A.P. (2005) Anoikis. *Cell Death Differ.*, **12**, 1473–1477.
35. Langenbach, K.J. and Rando, T.A. (2002) Inhibition of dystroglycan binding to laminin disrupts the PI3K/AKT pathway and survival signaling in muscle cells. *Muscle Nerve*, **26**, 644–653.
36. Munoz, J., Zhou, Y. and Jarrett, H.W. (2010) LG4-5 domains of laminin-211 binds alpha-dystroglycan to allow myotube attachment and prevent anoikis. *J. Cell. Physiol.*, **222**, 111–119.
37. Morgan, J.E. and Zammit, P.S. (2010) Direct effects of the pathogenic mutation on satellite cell function in muscular dystrophy. *Exp. Cell Res.*, **316**, 3100–3108.
38. Ross, J., Benn, A., Jonuschies, J., Boldrin, L., Muntoni, F., Hewitt, J.E., Brown, S.C. and Morgan, J.E. (2012) Defects in glycosylation impair satellite stem cell function and niche composition in the muscles of the dystrophic Large(myd) mouse. *Stem Cells*, doi: 10.1002/stem.1197.
39. Sacco, A., Mourkioti, F., Tran, R., Choi, J., Llewellyn, M., Kraft, P., Shkreli, M., Delp, S., Pomerantz, J.H., Artandi, S.E. and Blau, H.M. (2010) Short telomeres and stem cell exhaustion model Duchenne muscular dystrophy in mdx/mTR mice. *Cell*, **143**, 1059–1071.
40. Gensch, N., Borchardt, T., Schneider, A., Riethmacher, D. and Braun, T. (2008) Different autonomous myogenic cell populations revealed by ablation of Myf5-expressing cells during mouse embryogenesis. *Development*, **135**, 1597–1604.
41. Gregorevic, P., Allen, J.M., Minami, E., Blankinship, M.J., Haraguchi, M., Meuse, L., Finn, E., Adams, M.E., Frochner, S.C., Murry, C.E. and Chamberlain, J.S. (2006) rAAV6-Microdystrophin preserves muscle

function and extends lifespan in severely dystrophic mice. *Nat. Med.*, **12**, 787–789.
42. Yoshimura, M., Sakamoto, M., Ikemoto, M., Mochizuki, Y., Yuasa, K., Miyagoe-Suzuki, Y. and Takeda, S. (2004) AAV vector-mediated microdystrophin expression in a relatively small percentage of mdx myofibers improved the mdx phenotype. *Mol. Ther.*, **10**, 821–828.
43. Pacak, C.A., Walter, G.A., Gaidosh, G., Bryant, N., Lewis, M.A., Germain, S., Mah, C.S., Campbell, K.P. and Byrne, B.J. (2007) Long-term skeletal muscle protection after gene transfer in a mouse model of LGMD-2D. *Mol. Ther.*, **15**, 1775–1781.
44. Nathwani, A.C., Tuddenham, E.G., Rangarajan, S., Rosales, C., McIntosh, J., Linch, D.C., Chowdary, P., Riddell, A., Pie, A.J., Harrington, C. *et al.* (2011) Adenovirus-associated virus vector-mediated gene transfer in hemophilia B. *N. Engl. J. Med.*, **365**, 2357–2365.
45. Pane, M., Messina, S., Vasco, G., Foley, A.R., Morandi, L., Pegoraro, E., Mongini, T., D'Amico, A., Bianco, F., Lombardo, M.E. *et al.* (2012) Respiratory and cardiac function in congenital muscular dystrophies with alpha dystroglycan deficiency. *Neuromuscul. Disord.*, **22**, 685–689.
46. Kanagawa, M., Omori, Y., Sato, S., Kobayashi, K., Miyagoe-Suzuki, Y., Takeda, S., Endo, T., Furukawa, T. and Toda, T. (2010) Post-translational maturation of dystroglycan is necessary for pikachurin binding and ribbon synaptic localization. *J. Biol. Chem.*, **285**, 31208–31216.
47. Fukada, S., Yamaguchi, M., Kokubo, H., Ogawa, R., Uezumi, A., Yoneda, T., Matev, M.M., Motohashi, N., Ito, T., Zolkiewska, A. *et al.* (2011) Hesr1 and Hesr3 are essential to generate undifferentiated quiescent satellite cells and to maintain satellite cell numbers. *Development*, **138**, 4609–4619.
48. Segawa, M., Fukada, S., Yamamoto, Y., Yahagi, H., Kanematsu, M., Sato, M., Ito, T., Uezumi, A., Hayashi, S., Miyagoe-Suzuki, Y. *et al.* (2008) Suppression of macrophage functions impairs skeletal muscle regeneration with severe fibrosis. *Exp. Cell Res.*, **314**, 3232–3244.
49. Shin, J.H., Nitahara-Kasahara, Y., Hayashita-Kinoh, H., Ohshima-Hosoyama, S., Kinoshita, K., Chiyo, T., Okada, H., Okada, T. and Takeda, S. (2011) Improvement of cardiac fibrosis in dystrophic mice by rAAV9-mediated microdystrophin transduction. *Gene Ther.*, **18**, 910–919.

OPEN ACCESS Freely available online

PLOS ONE

Genome-Wide DNA Methylation and Gene Expression Analyses of Monozygotic Twins Discordant for Intelligence Levels

Chih-Chieh Yu[1☯], Mari Furukawa[1☯], Kazuhiro Kobayashi[1], Chizuru Shikishima[2], Pei-Chieng Cha[1], Jun Sese[3], Hiroko Sugawara[4], Kazuya Iwamoto[5], Tadafumi Kato[4], Juko Ando[6], Tatsushi Toda[1]*

1 Division of Neurology/Molecular Brain Science, Kobe University Graduate School of Medicine, Kobe University, Kobe, Japan, **2** Keio Advance Research Centers, Keio University, Tokyo, Japan, **3** Department of Computer Science, Graduate School of Information Science and Engineering, Tokyo Institute of Technology, Tokyo, Japan, **4** Laboratory for Molecular Dynamics of Mental Disorders, RIKEN Brain Science Institute, Saitama, Japan, **5** Department of Molecular Psychiatry, Graduate School of Medicine, The University of Tokyo, Tokyo, Japan, **6** Faculty of Letters, Keio University, Tokyo, Japan

Abstract

Human intelligence, as measured by intelligence quotient (IQ) tests, demonstrates one of the highest heritabilities among human quantitative traits. Nevertheless, studies to identify quantitative trait loci responsible for intelligence face challenges because of the small effect sizes of individual genes. Phenotypically discordant monozygotic (MZ) twins provide a feasible way to minimize the effects of irrelevant genetic and environmental factors, and should yield more interpretable results by finding epigenetic or gene expression differences between twins. Here we conducted array-based genome-wide DNA methylation and gene expression analyses using 17 pairs of healthy MZ twins discordant intelligently. *ARHGAP18*, related to Rho GTPase, was identified in pair-wise methylation status analysis and validated via direct bisulfite sequencing and quantitative RT-PCR. To perform expression profile analysis, gene set enrichment analysis (GSEA) between the groups of twins with higher IQ and their co-twins revealed up-regulated expression of several ribosome-related genes and DNA replication-related genes in the group with higher IQ. To focus more on individual pairs, we conducted pair-wise GSEA and leading edge analysis, which indicated up-regulated expression of several ion channel-related genes in twins with lower IQ. Our findings implied that these groups of genes may be related to IQ and should shed light on the mechanism underlying human intelligence.

Citation: Yu C-C, Furukawa M, Kobayashi K, Shikishima C, Cha P-C, et al. (2012) Genome-Wide DNA Methylation and Gene Expression Analyses of Monozygotic Twins Discordant for Intelligence Levels. PLoS ONE 7(10): e47081. doi:10.1371/journal.pone.0047081

Editor: Valerie W. Hu, The George Washington University, United States of America

Received February 9, 2012; **Accepted** September 11, 2012; **Published** October 17, 2012

Funding: This work was supported by Grant-in-Aid for Scientific Research on Innovative Areas (22129006 to TT) from the Ministry of Education, Culture, Sports, Science and Technology of Japan; by Grants-in-Aid for Scientific Research (S) (21223002 to JA and TT); by Scientific Research (B) (20390099 to TT); and by Challenging Exploratory Research (23650136 to KK) from the Japan Society for the Promotion of Science. The funders had no role in study design, data collection and analysis, decision to publish, or preparation of the manuscript.

Competing Interests: The authors have declared that no competing interests exist.

* E-mail: toda@med.kobe-u.ac.jp

☯ These authors contributed equally to this work.

Introduction

Individual differences in cognitive abilities have long been an intriguing phenomenon to both lay people and scientists. Differences in intelligence, as measured by IQ tests, appear to remain relatively stable from childhood to late life [1,2]. Further, the fact that intelligence, in the general population, has a normal distribution and long-term constancy allows for the assumption of the nature of IQ as being, at least partly, hereditary with quantitative trait features. In effect, the heritability of intelligence is estimated to be somewhere between 30% to over 80% in classical MZ twin versus dizygotic twin studies [3–5], marking it one of the highest among human quantitative traits.

Despite the significant role that genes are supposed to play in deciding an individual's cognitive abilities, progress to identify intelligence-related genes in healthy adults is not as promising [6,7], and contrasts the increasing list of some 300 genes associated with mental retardation [8]. One possible explanation for the lack of replicated genetic findings in normal-range intelligence is the small effect size of each gene. The fact that genome-wide association studies in the scale of thousands of subjects identified no specific genetic variants associated with human intelligence implies that very large sample sizes are necessary to detect individual loci [9].

As underpowered studies face challenges in the attempt to identifying small effect quantitative trait loci, twin research might provide an alternative. Twin studies serve more than a means to estimate heritability of the aforementioned complex traits; they also present an important resource to evaluate quantitative trait loci. There are accumulating evidences that long thought to be genetically identical MZ twins manifest variations in copy number [10] or point mutations limited to one twin [11]; however, these genomic discordances have failed to explain all phenotypic discrepancies [12]. Differences in phenotypes between MZ twins can possibly be attributed to environmental factors, as well as epigenetic variants, which refer to the gene expression-related modifications that occur without altering DNA sequences.

Epigenetic regulatory mechanisms have been reported to be associated with a number of biological phenotypes, including intelligence [13]. Among all known epigenetic mechanisms, DNA methylation has been the most extensively studied. Specifically, such studies have observed patterns of negative correlation between promoter region methylation and gene expression [14]. Additionally, studies based on phenotypically discordant MZ twins have revealed that those who are as best matched for genetics, gender, age, prenatal influences, and shared environment as nature could provide, are considered to possess the potential to detect epigenetic and transcriptomic differences, although research has yet to yield exclusive results [12,15].

In the present study, we recruited 17 healthy MZ twin pairs who manifested discordance for intelligence between co-twins (i.e., more than 1 standard deviation (SD)). Regarding that MZ twins are identical in genetic composition, the IQ difference could be associated with environmental factors, via epigenetic mechanisms regulations. By analyzing array-based genome-wide DNA methylation and gene expression profiles, a novel list of genes with functions related to protein synthesis, DNA helicase activities, and ion channels was generated. To our knowledge, this is the first study tested for epigenetic and expression differences between phenotypically normal, yet discordant, MZ twins via genome-wide approaches.

Results

General characteristics of participants

This study is a part of the Keio Twin Study project [16]. We have collected 240 MZ twin pairs with IQ scores of both siblings tested (Fig.S1). Seventeen MZ twin pairs (5 male pairs and 12 female pairs) aged 25.1±2.5 years (range, 21–31 years), with IQ scores of normal range yet manifesting significant between co-twins differences formed the present study sample (Table 1). Mean IQ score of all 34 participants was 100.91±13.32 (range, 67–139), while the mean difference between co-twins was 20.76 points (range, 15–45). No documented psychological or physiological conditions were noted at the time of recruitment. Since there is no standard definition of discordance in MZ twins IQ scores, we adopted 15-point-difference as the principle inclusion criterion. Fifteen-point is not only one standard deviation of IQ scores in general populations, but it is also the average IQ difference for genetically unrelated individuals sharing family environments, whereas identical twins differ by only about 6 IQ points on average [17].

27 genes identified by screening for epigenetically regulated candidate loci

We analyzed the methylation profiles of 25,500 human promoters utilizing methylated DNA enriched genomic DNA derived from peripheral blood cells. We used MAT (model-based analysis of tiling arrays) program [18] to identify genes that significantly differed between co-twins pairwisely. With a significance threshold set to $p<10^{-6}$, a total of 27 genes were recognized in 13 of the 17 twin pairs; however, none was shared in plural pairs (Table S1). In addition, a moderate positive correlation of 0.417 (Spearman's rank correlation coefficient, $p=0.048$) was found between the number of genes that epigenetically differed and pair-wise IQ differences (Fig. S2). On the other hand, after applying the log signal ratio (of the higher IQ twins to the lower IQ co-twins) to one-class t-test with the same significance threshold across all 17 twin pairs, we identified no locus manifesting significantly different methylation status.

Validation of *ARHGAP18* by bisulfite sequencing and quantitative RT-PCR

We performed a sodium bisulfite analysis to confirm the methylation status at the 27 gene loci putatively identified as being differentially methylated. After sequencing at least 30 clones for each locus, statistically significant difference in methylation status between co-twins was validated on two genes, *ARHGAP18* (Rho GTPase activating protein 18, $p=5.12806\times10^{-8}$; chi-square test) and *OR4D10* (olfactory receptor 4D10, $p=0.0234658$; chi-square test) (Fig. 1A and B).

After confirmation of methylation status, we correlated the data with their expression levels using total RNA derived from lymphoblast cell lines by qRT-PCR. The observed reduction in DNA methylation status of *ARHGAP18* was correlated with its increased expression level in the subject with lower IQ scores of the twin pair from which the gene was identified (2.04 fold, $p=0.024767$; Mann-Whitney U test) (Fig. 1C, left graph). Increased transcription levels were observed after a 3-day treatment of the demethylating agent 5-aza-2-deoxycytidine (5-azadC), and the difference between the twins was eliminated, suggesting that the expression is regulated by the methylation of the promoter (Fig. 1C, right graph). Meanwhile, no expression of *OR4D10* could be detected in the lymphoblast cell lines.

No gene manifesting statistically significant differences between the group of twins with higher IQ and that of their co-twins after the expression array analysis

Apart from the epigenetic approach described above, we used an expression microarray analysis to directly compare the genome-wide gene expression profiles of the higher IQ twins versus their lower IQ co-twins. At first, principal component analysis (PCA) was performed to facilitate visualization of the relationships between groups (Fig. S3). As a result, the two groups compositing twins with higher or lower IQ scores could not be readily distinguished. Likewise, the dendrograms, produced by hierarchical clustering, also failed to demonstrate differences in general expression patterns between these two phenotypic groups (Fig. S4). Next, ANOVA analysis was applied to identify whether there were differentially expressed genes between these two groups; however, no gene met the criteria of a FDR (false discovery rate)-adjusted p of 0.05. A one-class t-test analysis with multiple sample correction was conducted across all log ratios. Similarly, no significantly differentially expressed gene was identified.

Candidate genes list resulted from direct pair-wise comparison of the expression array data

Next, we applied a direct pair-wise comparison to focus on the genes up-regulated in the same tendency. Fold-change values of the expression levels of all genes were first calculated for each twin pair, from which genes with a fold-change value more than 2 were included (Dataset S1). We then generated a list of candidate genes by picking up those replicated in most twin pairs (Table 2). *UCHL1* (ubiquitin carboxyl-terminal esterase L1), along with the other 7 genes, were found to have higher expression levels in the higher IQ twins of at least 4 pairs, while 6 genes were up-regulated in some lower IQ twins.

Identification of 3 genes with borderline significance by grouping samples according to individual gene expression level

To further increase the possibility of identifying candidate genes, we performed an analysis based on individual gene expression level. After dividing the twin siblings of each pair into

Table 1. Background data for participants.

Twin Pair ID	Age (year)	Gender	IQ Scores* (Points)		IQ score differences
			Twin A	Twin B	
1	31	F	99	82	17
2	30	F	110	91	19
3	22	M	82	112	−30
4	20	F	100	78	22
5	29	F	90	108	−18
6	20	F	86	104	−18
7	24	F	93	76	17
8	25	F	126	106	20
9	21	M	97	80	17
10	27	F	123	104	19
11	22	F	93	108	−15
12	23	M	97	117	−20
13	27	M	121	139	−18
14	23	M	126	108	18
15	26	F	112	67	45
16	26	F	108	90	18
17	24	F	110	88	22

*IQ scores calculated after participants took the full version of Kyodai Nx15- test.

doi:10.1371/journal.pone.0047081.t001

higher and lower expression groups according to the expression level of every gene, a paired t-test was carried out to determine if there was a significant difference between the mean IQ scores of the two groups. Whereas not a single gene reached the corrected cutoff p of 10^{-6}, 3 genes, *RFK* (riboflavin kinase), *RPL12* (ribosomal protein L12), and *RMRP* (RNA component of mitochondrial RNA processing endoribonuclease), manifested borderline significance (Fig. 2). The twins manifesting up-regulated expression level of *RFK* showed the tendency to have lower IQ scores than their co-twins, while *RPL12* and *RMRP* might likely to contribute to higher intelligence.

Identification of 4 differentially expressed gene sets by GSEA

It remained possible that functionally-related genes might have important gene expression changes in a set-wise matter without any individual transcript meeting the criteria of significance. Using GSEA [19] under the cutoff FDR q-value of <0.25, we denoted 1 and 4 up-regulated gene sets from KEGG and Gene Ontology (GO) database respectively in the group of higher IQ twins, while 1 gene set each from KEGG and Reactome pathway database was found to be up-regulated in the group of lower IQ twins (Table S2 and Fig. 3). From the results employing GO database, the leading edge analysis revealed 8 genes (*MRPS35*, *MRPL23*, *MRPL52*, *MRPL41*, *MRPL12*, *MRPS15*, *MRPS22*, and *MRPL55*) with core enrichment in the gene sets "Organellar Ribosome," "Ribosomal Subunit," and "Mitochondrial Ribosome", whereas the fourth gene set "ATP-dependent DNA Helicase Activity" was comprised of 7 other genes (*XRCC5*, *XRCC6*, *DHX9*, *PIF1*, *G3BP1*, *RUVBL2*, and *CHD4*) with core enrichment. By utilizing Reactome database, all 6 genes from the gene set "Reactome CREB phosphorylation through the activation of CAMKII" were enriched.

A different approach was carried out to the same end. Specifically, we performed a GSEA on each twin pair. Depending on the twin pairs analyzed and pathway databases used, as many as 284 gene sets were found to be significantly different between the siblings (Dataset S2, S3, S4, S5). Gene sets replicated in most twin pairs were listed. In general, pathways related to DNA replication, ribosomes, and proteases were found in higher IQ twins of most twin pairs, while cell signaling associated ones tended to be up-regulated in lower IQ twins (Table 3). In order to focus on those genes which effectively contributed to the enrichment of each given gene set, we first generated up- and down-regulated leading edge subsets for each twin pair, and then extracted those genes that were nominated most often across plural twin pairs (Table 4). Up-regulation of *IGF1* was found in the higher IQ twins of 4 pairs, whereas potassium channel-coding genes *KCNE2* and *KCNQ3*, along with an acetylcholine receptor-coding gene *CHRNA2* manifested higher expression levels in some lower IQ twins. Among all the candidates, *IGF1* was selected for further analysis for its important role in growth and development [20]. We performed bisulfite sequencing of the promoter regions for the 4 twin pairs manifesting an up-regulated expression level in the higher IQ siblings. However, no significant differences were noted in the methylation status of the 2 promoter domains (P1 and P2) between the siblings (Table S3).

Discussion

Given that the concept of general cognitive ability, designated as *g*, has been widely accepted to depict a near-universal positive covariation among diverse measures of cognitive abilities, naming even one genetic locus that is reliably related with normal-range intelligence remains challenging [21]. IQ is easy to quantify and compare among different individuals. Although not conclusively, the substantial *g*-loading for IQ [22] justifies its role to represent the general intelligence levels. Benefiting from the extraordinary similarities in genomic constitution and environmental factors,

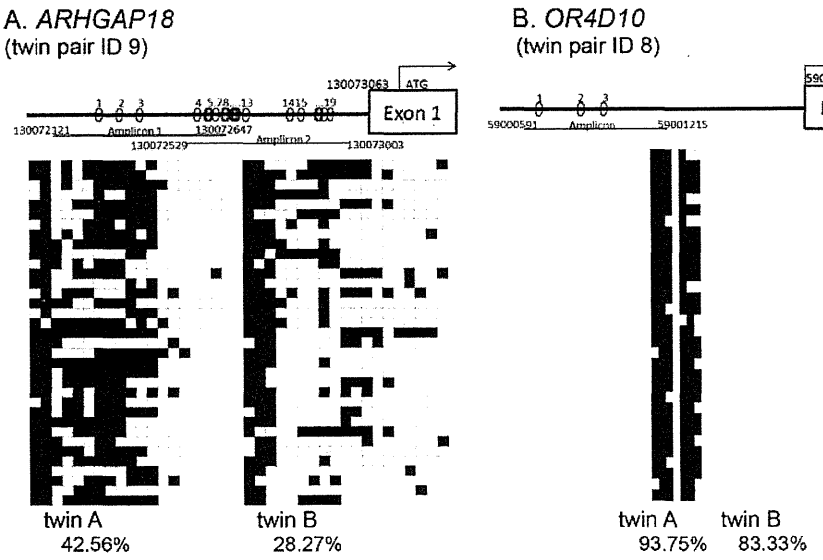

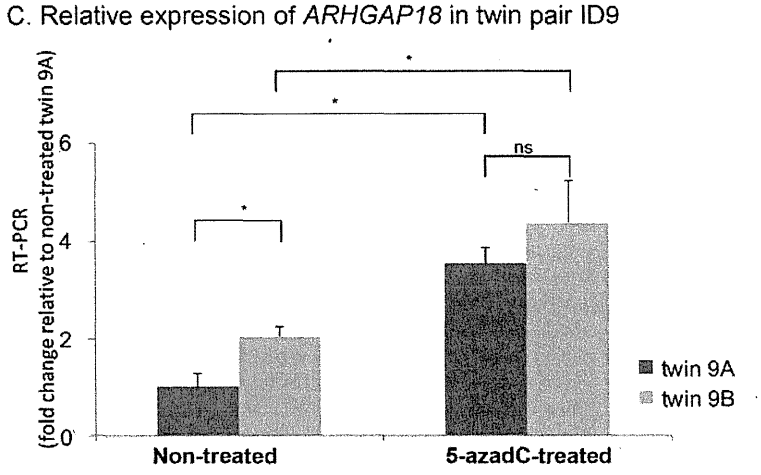

Figure 1. DNA methylation status of the 5′-regions of *ARHGAP18* and *OR4D10* analyzed by bisulfite sequencing along with the quantitative RT-PCR analysis for *ARHGAP18* expression. A, B. DNA methylation status analyzed by bisulfite sequencing. Schematic representation (top) for the relative position of CpGs within amplified regions and methylation profiling by bisulfite sequencing (bottom). The numbers at the ends of amplicons indicate the genome coordinates relative to the NCBI Build 36 genome assembly. Of all 27 loci identified by screening for epigenetically regulated candidate genes, A. *ARHGAP18* and B. *OR4D10* were validated by direct bisulfite sequencing. At least 30 clones were sequenced for each locus. Open squares indicate unmethylated CpG nucleotides and closed squares indicate methylated ones. Rows indicate the methylation status of each colony sequenced, while columns indicate the positions of CpG nucleotides.The percentages below refer to the ratio of CpG methylation. C. qRT-PCR analysis of *ARHGAP18* mRNA relative to *GAPDH* in the twin pair ID 9. *ARHGAP18* expression in twin 9A untreated with 5-azadC was normalized to 1. Error bars indicate ± SD. *P*-value was calculated using Mann-Whitney U test with asterisks indicating statistical significance ($p<0.05$). ns: not significant.
doi:10.1371/journal.pone.0047081.g001

studies based on discordant monozygotic twins, even with limited sample size (as small as 20–50 twin pairs), are capable of uncovering phenotype-associated epigenetic changes independent of underlying sequence variance [23]. By successfully recruiting 17 pairs of identical twins discordant for intelligence levels, we shall have a modest power in the identification of intelligence-related epigenetic differences. To our knowledge, this is the first genome-wide methylation and gene expression study administering the characteristics of monozygosity to access the epigenetic and expression changes for a quantitative trait.

Researchers have reported that patterns of epigenetic modifications in MZ twins diverge as they age [24]. Provided that all 17 twin pairs in this study were in early adulthood, it might not be surprising that only few loci revealed significant differences in methylation status. Of the 27 candidate loci nominated by promoter-arrays-based methylation analyses, bisulfite sequencing successfully validated only 2 genes. One explanation of the discrepancy between these two methods is that we adopted a less stringent criterion of *p*-value (10^{-6}, instead of a Boferroni corrected p-value of 10^{-8} considering that GeneChip Human

Table 2. List of genes having the same tendency of expression level in most twin pairs.

Up-regulated in co-twins with	Gene	Shared by twin pair ID
Higher IQ scores	*GTSF1*	1,2,7,11,14,15,16
	AK3L1	1,3,9,11,17
	PRKCH	2,9,11,14,17
	CDRT1	2,9,10,11,14
	LRIG3	1,2,9,15
	VSIG6	2,10,11,13
	SNORA20	3,6,10,12
	UCHL1	8,9,11,15
Lower IQ scores	*CD96*	1,2,4,9,14
	CXCL10	1,6,9,11
	CDC42BPA	1,2,6,9
	CXCR4	1,2,6,14
	EPS8	2,9,10,16
	FAM169A	3,9,11,15

doi:10.1371/journal.pone.0047081.t002

Promoter 1.0 Array contains 4.6 million probes). As a result, we were able to detect more candidate loci from the practically congruent MZ twin samples, only at the expense of precision rate. The technical limitations of MethylMiner collection might also contribute to false positives. After bisulfite sequencing and qRT-PCR validation, we identified one candidate gene, *ARHGAP18*, which encodes one of the Rho GTPase-activating proteins (GAPs) that modulate cell proliferation, migration, intercellular adhesion, cytokinesis, proliferation differentiation, and apoptosis [25]. Mutations in a handful of Rho-linked genes were documented to be associated with X-linked mental retardation [8], by which the importance of GAP activity in normal neuronal functions was proposed [26]. Notwithstanding the identification of *ARHGAP18* in a genome-wide association study for schizophrenia [27], it had not been previously connected to cognitive abilities until the present study.

We were not able to identify a single gene that displayed significantly different expression level between the group of twins with higher IQ scores and their co-twins. From the list of candidate genes generated by direct pair-wise comparison, UCHL1 is a brain-specific de-ubiquitinating enzyme. While the substrates are still unknown, loss of its enzyme activity has been reported in neurological diseases such as Alzheimer's disease and Parkinson's disease [28]. In a different approach, *RFK*, *RPL12*, and *RMRP* showed borderline significance. *RFK* encodes riboflavin kinase, an essential enzyme to form flavin mononucleotide, is important in a wide range of biological metabolisms [29]. *RPL12* encodes a ribosomal protein of the 60S subunit, while *RMRP* encodes the RNA component of mitochondrial RNA processing endoribonuclease. Although none of these 3 genes had ever been connected with cognitive functions, it remains possible that their biophysical characteristics might become more pronounced in cells having as high a metabolic rate as neurons.

In the gene set based approach, GSEA of between-group and between co-twin comparisons revealed several mitochondrial ribosomal protein-coding genes. Mitochondria, which are responsible for most of the energy requirement for cellular metabolism, have their own translation system for the 13 proteins essential for oxidative phosphorylation in mammals. All 78 human mitochondrial ribosome proteins are translation products of nuclear genes, of which some were identified as candidate genes for several congenital diseases [30]. No exclusive conclusion about the connection of mitochondrial ribosomal function and cognitive ability could be drawn before being further validated. Nevertheless, we hypothesized that, for the highly differentiated and high energy-demanding central nervous system, essential proteins for

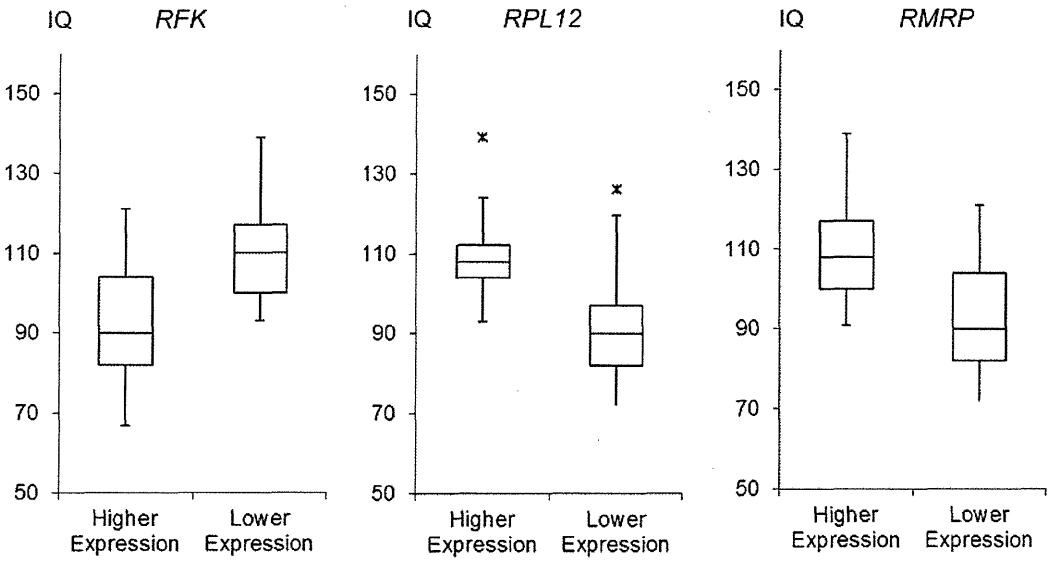

Figure 2. Three genes manifesting borderline significance by grouping samples according to individual gene expression level. IQ scores in subjects were grouped according to the relatively higher (Higher Expression) or lower (Lower Expression) expression levels within each twin pair. Three genes, *RFK*, *RPL12*, and *RMRP*, manifested the smallest p yet failed to meet the cutoff value of $p = 10^{-6}$. Data are presented as box plots (minimum, 25% quartile, median, 75% quartile, maximum). The red asterisks indicate maximum outliners.
doi:10.1371/journal.pone.0047081.g002